공학석사 학위논문

Development of Prediction Models of Ship Power and Ocean Environmental Data Based on Deep Learning

딥 러닝을 이용한 해기상 및 소요 마력 예측 모델 개발

2021년 2월

서울대학교 대학원
조선해양공학과
이 준 범

Development of Prediction models of Ship Power and Ocean Environmental Data based on Deep Learning

딥 러닝을 이용한 해기상 및 소요 마력 예측 모델 개발

지도 교수 노 명 일

이 논문을 공학석사 학위논문으로 제출함

2021년 2월

서울대학교 대학원

조선해양공학과

이 준 범

이준범의 공학석사 학위논문을 인준함

2021년 2월

위 원 장 김태완 (인)

부위원장 노명일 (인)

위 원 우종훈 (인)

Contents

Figures

Tables

Abstract

Development of Prediction Models of Ship Power and Ocean Environmental Data Based on Deep Learning

June-Beom Lee

Naval Architecture and Ocean Engineering

The Graduate School

Seoul National University

In order to determine an economical route that minimizes the ship's required power, it is necessary to predict the sea level and the ship's required power accordingly. The weather forecasting companies such as the European Center for Medium-Range Weather Forecast (ECMWF) and Hybrid Coordinate Ocean Model (HYCOM), which provide ocean environmental data, typically make short-term forecasts of around six weeks. Therefore, when a long-term prediction is needed, it is necessary to predict ocean environmental data

on its own. In the case of the prediction of ship's requird power, a numerical method using model test results is traditionally used. However, this method is difficult to accurately predict the ship's required power due to the model test's uncertainty. To solve this problem, an onboard test must be conducted, but this is expensive and time-consuming. Therefore, in this study, the ocean environmental data and ship's required power were predicted using deep learning.

In relation to the prediction of ocean environmental data, many studies have used deep learning. However, most of them made predictions for limited ocean environmental data such as wave height, wave period, and wave direction. In addition, there was a limitation in that prediction was made for a specific sea area rather than the entire sea area. Therefore, in this study, the ocean environmental data of the entire sea area was imaged for prediction. In addition, convolutional LSTM suitable for training time-series image data was utilized. In addition, AutoEncoder was used to solve delayed prediction that mainly occurs in the problem of prediction of time series data. Also, to find the optimal model, the performance of the model was evaluated by changing the size of input data (look back step) and prediction time of output data (look forward step). Finally, based on this model, the entire sea area was divided into 12 areas, and the prediction of ocean environmental data was carried out.

Regression analysis was used in many studies related to the prediction of a ship's required power. However, the regression analysis showed limitations in the accuracy of prediction in the case of complex problems such as the prediction of the ship's required power affected by maritime and ship operating conditions. Therefore, in this study, deep feedforward neural network (DFN), a deep learning model suitable for numerical prediction, was used. In addition, various methods were used to increase prediction

accuracy. First, in the case of wind and wave-related data in ocean environmental data, the effect was confirmed by performing pre-processing with relative values for the ship. Second, the effect was confirmed by changing the DFN model structure according to the characteristics of the DFN input data. Third, we analyzed the prediction accuracy according to the combination of five hyperparameters: number of hidden layers, number of hidden nodes, learning rate, dropout, and gradient optimizer for the DFN learning model. Fourth, k-means clustering was conducted to develop an independent model for predicting the ship's required power according to a sea state and ship operational conditions. As described above, the performance of various prediction models was compared and analyzed.

Keywords: Ocean environmental data, ship's required power, DFN (Deep Feedforward Neural network), Convolutional LSTM (Long Short-Term Memory), AutoEncoder

Student number: 2018-24953

1. Introduction

1.1. Research background

In order to determine an economical route that minimizes the ship's required power, it is necessary to predict the ocean environmental data and the ship's required power. Weather forecasting companies such as the European Center for Medium-Range Weather Forecast (ECMWF) and Hybrid Coordinate Ocean Model (HYCOM), which provide ocean environmental data, typically make short-term forecasts of around six weeks. Therefore, when the long-term prediction is needed, it is necessary to predict ocean environmental data on its own. Also, in the case of the prediction of the ship's required power, the method suggested in ISO 15016 (ISO 15016, 2015) is widely used. However, this method is not suitable to be applied to actual ships because it is a method made for correction of the commissioning speed. Also, traditionally, numerical methods have been used to predict the ship's required power. However, this method has limitations in predicting a realistic ship's required power due to the uncertainty when expanding the model test results to the actual ship. Therefore, recently, a data-driven approach is mainly used. The data-driven approach is mainly regression method and deep learning. The regression method is a method of linearly grasping the correlation between several variables. Next, deep learning is a type of machine learning based on artificial neural networks, which is an effective method for identifying data patterns. The complex model structure can be tuned, so it is more effective in identifying patterns of complex problems compared to the regression method. Deep learning can be classified into various models according to data characteristics and problems. In the case of oceanographic data prediction, since it can be classified as a problem of prediction of time series, RNN (Rumelhart et al., 1986) is mainly used in this regard. In addition, since

the prediction of the ship's required power can be classified as a numerical data prediction problem, DFN (Werbos, 1974) is mainly used in this regard. In this study, deep learning was used to predict ocean environmental data and required horsepower. Figure 1 shows the necessity of this study.

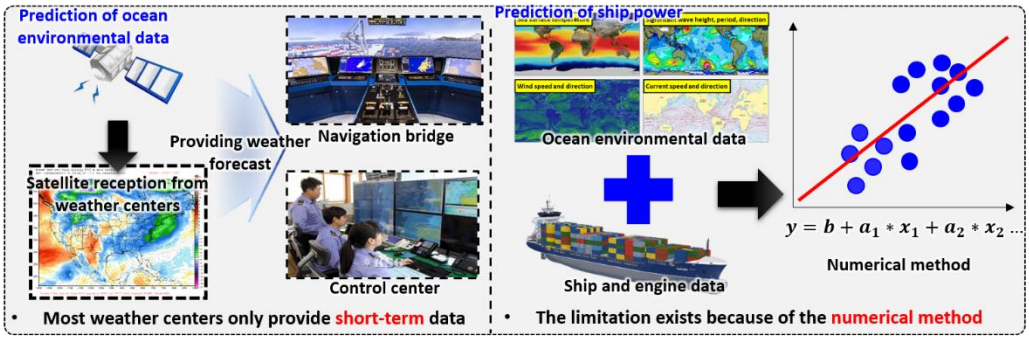

Figure 1. The necessity of this study

Table 1. Related works

1) DFN: Deep Feedforward Network / 2) GP: Genetic Programming / 3) MT: Model Trees /

4) ANFIS: Adaptive-Network-based Fuzzy Inference System / 5) FIS: Fuzzy Inference System / 6) SST: Sea Surface Temperature / 7) LSTM: Long Short-Term Memory / 8) MLP: Multi-Layer Perceptron / 9) SVM: Support Vector Machine / 10) BHP: Brake Horse Power

Related study	**Purpose of study**	**Prediction method**	**Input data**
Rakke (Rakke, 2016)	Estimating ship emission using Holtrop-Mennen method	Holtrop-mennen method	Automatic identification system (AIS) data, world fleet data, ship & engine data
Kristensen et al. (Kristensen and Lützen, 2012)	Estimating ship power using Harvald method	Harvald method	Ship data
Yoo et al. (Yoo and Kim, 2017)	Estimating ship power using a linear regression method	Linear regression method	Ship & engine data, ocean environmental data
Uyanik et al. (Uyanik et al., 2019)	Estimating fuel oil consumption (FOC) using a multi-linear regression method	Multi-linear regression method	Ship & engine data, ocean environmental data
Mahjoobi et al. (Mahjoobi and Kazeminezhad, 2008)	Comparing and estimating wave height, wave period, wave direction derived from various deep learning models	DFN model ANFIS[4)] FIS[5)]	Wind direction, wind speed, fetch length, wind duration
Gunaydin et al. (Gunaydin, 2008)	Estimating wave height using ANN model	DFN model	Wind speed, sea level pressure, air temperature

Zhang et al. (Zhang et al., 2017)	Estimating SST[6] using LSTM model	LSTM[7] model	SST
James et al. (James et al., 2018)	Estimating wave height and wave period using MLP[8], SVM[9] model	MLP model SVM model	Wave height, wave period, wave direction, Wind speed, current speed
This project	Estimating wave height, wave period, wave direction, SST, wind speed, wind direction, current speed, current direction using LSTM, Convolutional LSTM model. Estimating BHP[10] using DFN	DFN model LSTM model Convolutional LSTM model	wave height, wave period, wave direction, SST, wind speed, wind direction, current speed, current, current direction, BHP, ship heading, ship speed

1.2. Related works

Table 1 summarizes and summarizes related studies. First, in the case of the prediction of the ship's required power, the numerical method using the model test results was used a lot. Rakke (Rakke, 2016) calculated the ship's resistance using the Holtrop-Mennen method (J and G, 1982), calculated the ship's required power through this, and finally predicted the ship emission. Kristensen et al. (Kristensen and Lützen, 2012) predicted the ship's resistance and the ship's required power using the Harvald method (Harvald, 1992). However, this method has a limitation in that the prediction accuracy is degraded due to the error of the model test result and the uncertainty in the expansion process to the actual ship. Therefore, in recent years, the regression method is mainly used to predict the ship's required power. Yoo et al. (Yoo and Kim, 2017) predicted the ship's speed using the linear regression method and then used this to predict the required horsepower. Uyanik et al. (Uyanik et al., 2019) predicted fuel consumption using the multi-linear regression method. However, the more complicated the regression method is, the less accurate it is, so there is a limitation in predicting the required horsepower affected by the ship's operating conditions and sea conditions.

In the case of prediction of ocean environmental data, deep learning was used a lot. Mahjoobi et al. (Mahjoobi and Kazeminezhad, 2008) predicted wave height, wave period, and wave direction using deep feedforward neural network (DFN), a basic deep learning model. Gunaydin et al. (Gunaydin, 2008) proposed a model that predicts wave height using DFN. Zhang et al. (Zhang et al., 2017) predicted water temperature using Long Short-Term Memory (LSTM), a deep learning model that considers the characteristics of time series data. James et al. (James et al., 2018) proposed a model that predicts wave height and wave

period using the multi-layer perceptron (MLP) and support vector machine (SVM).

However, this method has a limitation in that it is difficult to predict the entire sea area because it predicts ocean environmental data for an area, not the entire sea area. Therefore, in this study, the ocean environmental data was imaged to the prediction for the entire sea area, and a prediction model of ocean environmental data was developed using effective convolutional LSTM (Shi et al., 2015). Also, to predict the ship's required power, a required horsepower prediction model was developed using DFN, which is mainly used for predicting numerical data. Using the finally developed sea weather prediction model and required horsepower prediction model, a program was developed to predict the sea level in the sea area near the route and predict the required horsepower when a route is given. Figure 2 shows the structure of this study.

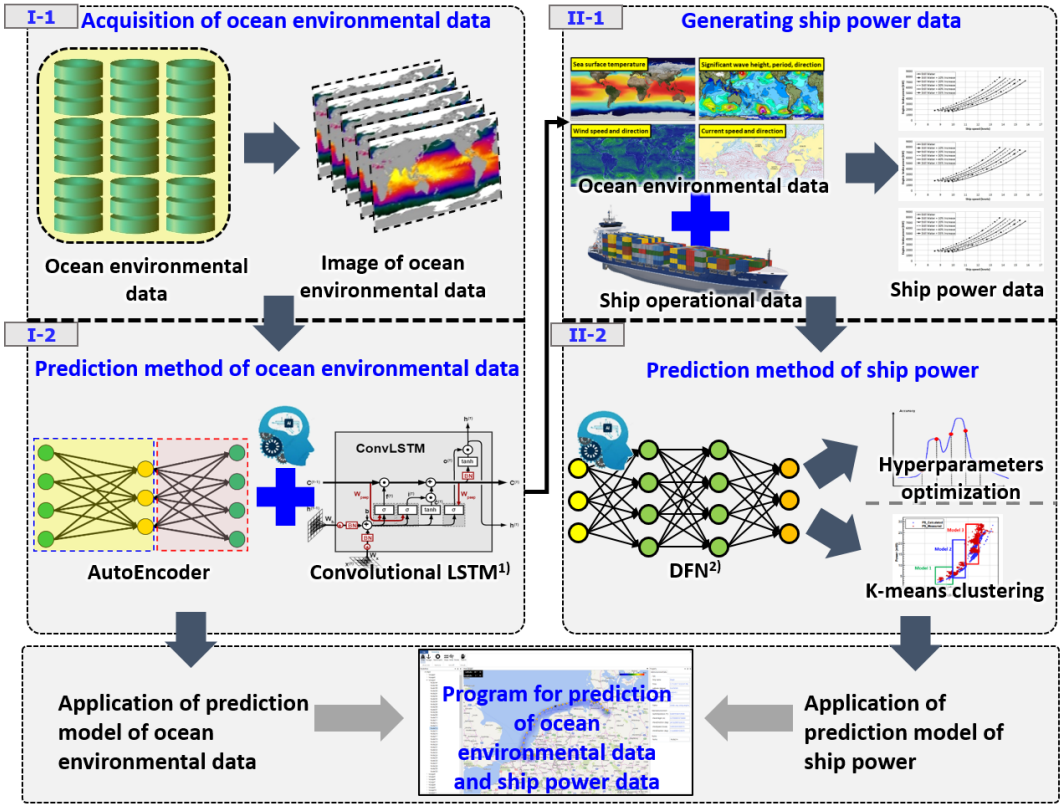

Figure 2. Configuration of this study

2. Prediction method of ocean environmental data

In this study, a model for predicting ocean environmental data was proposed to determine an economical route. Data for marine weather forecasting were obtained from meteorological centers of the European Center for Medium-Range Weather Forecast (ECMWF), National Oceanic and Atmospheric Administration (NOAA), and Hybrid Coordinate Ocean Model (HYCOM). Convolutional LSTM, which is used for predicting image time series data among deep learning models, was used as a model for predicting sea weather. Eight types of sea weather data (wave height (SWH), wave period (MWP), wave direction (MWD), wind speed-u (u component), wind speed–v (v component), current speed-u (u component), current) using deep learning models speed-v (v component)) was predicted. In addition, outliers of the ocean environmental data were removed by using AutoEncoder, and prediction accuracy was improved through this. This section introduces the entire process from acquisition of ocean environmental data to convolutional LSTM and AutoEncoder.

In order to predict the ship's required power, eight types of ocean environmental data are required: water temperature, wave height, wave direction, wave period, wind speed, wind direction, current speed, and current direction. Companies that provide ocean environmental data include ECMWF (European Center for Medium-Range Weather Forecast), NOAA (National Oceanic and Atmospheric Administration), and HYCOM (Hybrid Coordinate Ocean Model). Since ECMWF provides data on wave height, wave period, wave direction, wind speed, wind direction, etc., including water temperature not provided by NOAA, and HYCOM provides data on current speed and current direction,

ECMWF and HYCOM provide ocean environmental data. Twenty years of ocean environmental data were extracted from ECMWF, and four years and four months of ocean environmental data were extracted from HYCOM using the Python code developed in-house. Table 2 summarizes the agencies that provide ocean environmental data.

Table 2. Provider of ocean environmental data

	ECMWF	**NOAA**	**HYCOM**
Provided data	SST, wind speed, wind direction, wave height, wave period, wave direction, etc.	Wind speed, wind direction, wave height, wave period, wave direction, etc.	SST, current speed, current direction, sea level
Position resolution	Every 0.125 degrees (about 17km)	Every 0.5 degrees (about 56km)	Every 0.08 degrees (about 9km)
Time interval	Every 6 hours	Every 1 hour	Every 6 hours

2.1. Prediction model of ocean environmental data

2.1.1. LSTM

Ocean environmental data has the characteristics of time series data, and it is necessary to create and train a deep learning model suitable for it. In the case of a general deep learning model, it is suitable for predicting simple numerical data, but it is difficult to reflect time-series characteristics because the hidden layer is independently learned. RNN was developed to compensate for the shortcomings of this deep learning model and to consider time series characteristics. RNN is a neural network in which the hidden layer receives the previous state value and is an effective deep learning model when dealing with time-series data because past data affect the current output. However, in the case of RNN, when the

period of the input data is long, a vanishing gradient problem occurs in which the gradient decreases rapidly when the backpropagation, a process of updating the weight, is performed. To prevent this, a prediction model using LSTM was developed.

LSTM is a type of RNN that is useful when training patterns of time series data, and is a model designed to solve the vanishing gradient problem. Unlike RNN, where the hidden state is simply multiplied, LSTM contains a forget gate that determines how much of the previous state is reflected and an input gate that determines how much of the current state is reflected, thereby solving the vanishing gradient problem. Figure 3 shows the structure of LSTM.

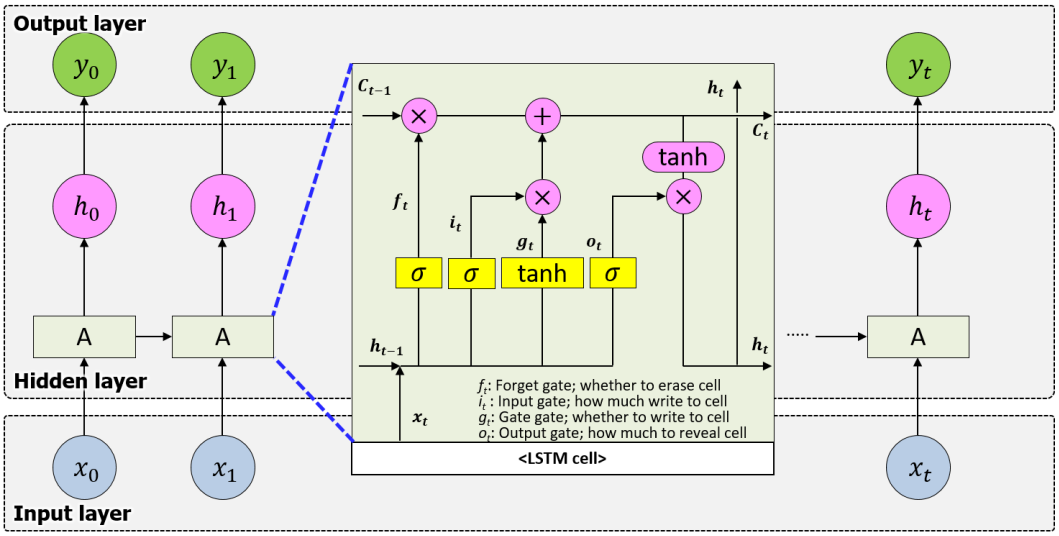

Figure 3. Configuration of LSTM

As can be seen in the cell structure, it is more complex than the general structure of RNN. Equations (1)–(6) show the formula of LSTM.

$$f_t = \sigma(W_{xf} x_t + W_{hf} h_{t-1} + b_f) \quad (1)$$

$$i_t = \sigma(W_{xi} x_t + W_{hi} h_{t-1} + b_i) \quad (2)$$

$$o_t = \sigma(W_{xo} x_t + W_{ho} h_{t-1} + b_o) \quad (3)$$

$$g_t = \tanh(W_{xg} x_t + W_{hg} h_{t-1} + b_g) \quad (4)$$

$$c_t = f_t \odot c_{t-1} + i_t \odot g_t \quad (5)$$

$$h_t = o_t \odot \tanh(c_t) \quad (6)$$

In Equations (1)–(6), σ is the sigmoid function, W is the weight of each layer, x_t is the input data, and b is the bias. In equations (5) and (6), $\odot$ is the Hadamard product. f_t is a gate that reflects past data to cell state, $i_t \odot g_t$ is a gate that reflects current data to cell state.

2.1.2. Convolutional LSTM

LSTM is a model that receives and predicts ocean environmental data at a specific point as one-dimensional time series data. In order to predict the ocean environmental data for all sea areas, it is necessary to develop a prediction model for all latitude and longitude

points. However, it is difficult in reality using LSTM. Therefore, when the ocean environmental data of the sea area is imaged, it is possible to predict ocean environmental data of the sea area with a single model. Convolutional LSTM is a model designed to predict time series characteristics of image data. It is similar to LSTM in that it is useful for grasping the pattern of time series data, but the difference is that an image is input to each node and is multiplied by convolution. By using Convolutional LSTM, it is possible to image the entire ocean environmental data in the sea area and predict it with a single model. Figure 4 shows the configuration of convolutional LSTM.

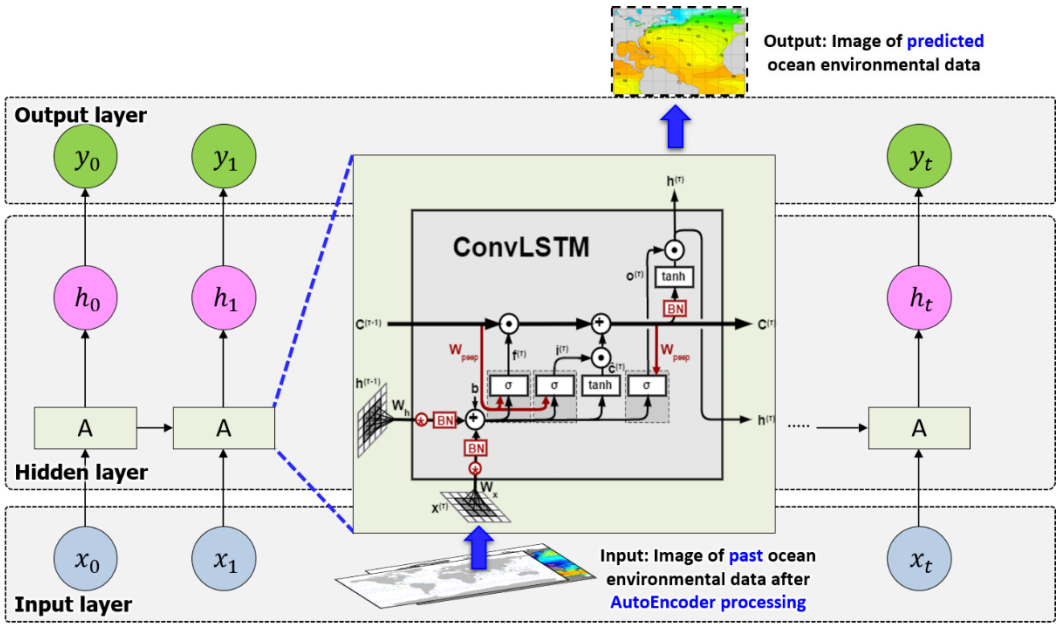

Figure 4. Configuration of convolutional LSTM

As can be seen from the cell structure, it is similar to LSTM. However, the image is input, and convolution product is used for calculation. Equations (7)–(12) show the formula of convolutional LSTM.

$$f_t = \sigma(W_{Xf} * X_t + W_{Hf} * H_{t-1} + W_{cf} \odot C_{t-1} + b_f) \tag{7}$$

$$i_t = \sigma(W_{Xi} * X_t + W_{Hi} * H_{t-1} + W_{Ci} \odot C_{t-1} + b_{Hi}) \tag{8}$$

$$g_t = \tanh(W_{Xg} * X_t + W_{Hg} * H_{t-1} + b_{h\_g}) \tag{9}$$

$$C_t = f_t \odot C_{t-1} + i_t \odot g_t \tag{10}$$

$$o_t = \sigma(W_{Xo} * X_t + W_{Ho} * H_{t-1} + W_{Co} \odot C_t + b_{h\_o}) \tag{11}$$

$$H_t = o_t \odot \tanh(C_t) \tag{12}$$

In Equations (7)-(12), X is the input data of the image, and * is the convolution product.

2.2. AutoEncoder

A common problem when predicting time series data using LSTM is delayed prediction. The delayed prediction problem is a problem of predicting by scaling input data closest to the ground truth (answer) without making a correct prediction when it is difficult to identify a data pattern. Since time series data is predicted by scaling at every

time point, the prediction trend looks like the result of shifting the graph of the actual time series data. Figure 5 shows an example of a delayed prediction problem. As a result of predicting the SST after 30 days, delayed prediction clearly occurred. In this way, the delayed prediction problem does not identify the pattern of data but derives prediction results by cheating input data.

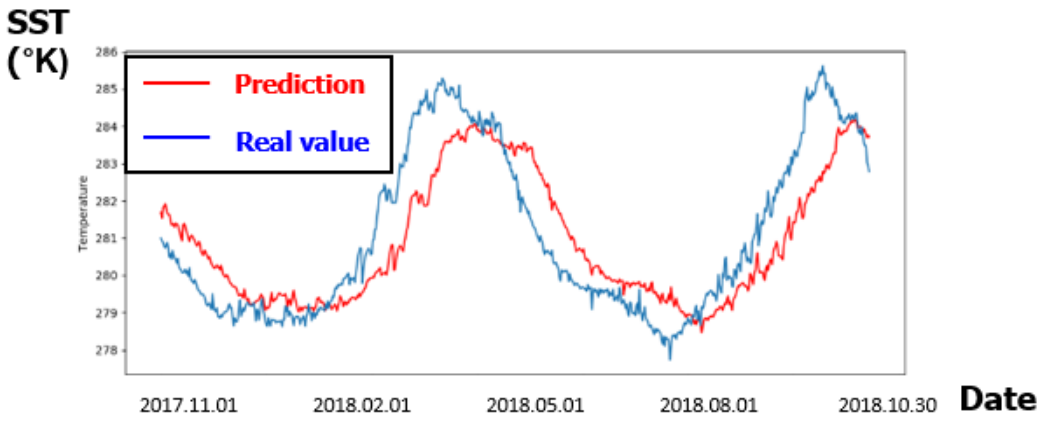

Figure 5. Example of delayed prediction

In order to understand the cause of the delay prediction problem, STL decomposition was performed on the ocean environmental data. STL decomposition is a method of classifying time series data into a trend representing an increase or decrease, seasonality representing a repetitive pattern, and noise, a random component. Figure 6 shows the result of STL decomposition.

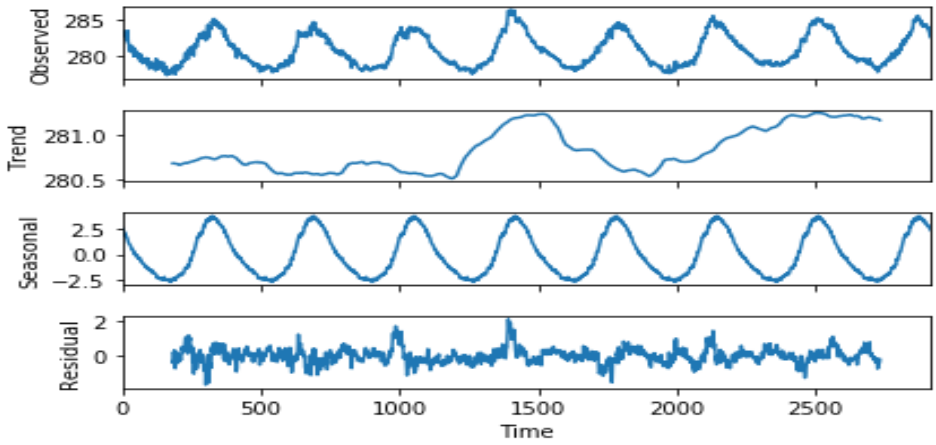

Figure 6. Result of STL decomposition

As a result of training about each element, it was confirmed that the pattern of noise was not identified. Therefore, we concluded that noise is the cause of delayed prediction because the time series data pattern cannot be recognized. Figure 7 shows the result of learning about the noise. As can be seen from Figure 7, it can be seen that it is not possible to train noise accurately.

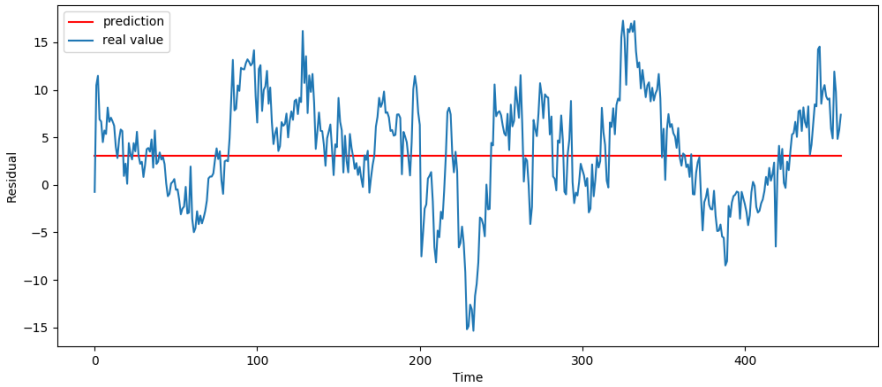

Figure 7. Training result of noise

To solve the delay prediction problem, it was previously confirmed that noise removal of data is necessary. AutoEncoder (Kramer, 1991) is a representative method of removing noise in an end-to-end method in a deep learning model. AutoEncoder removes noise by extracting meaningful features through an encoder and reconstructing them through a decoder. Figure 8 shows the configuration of AutoEncoder.

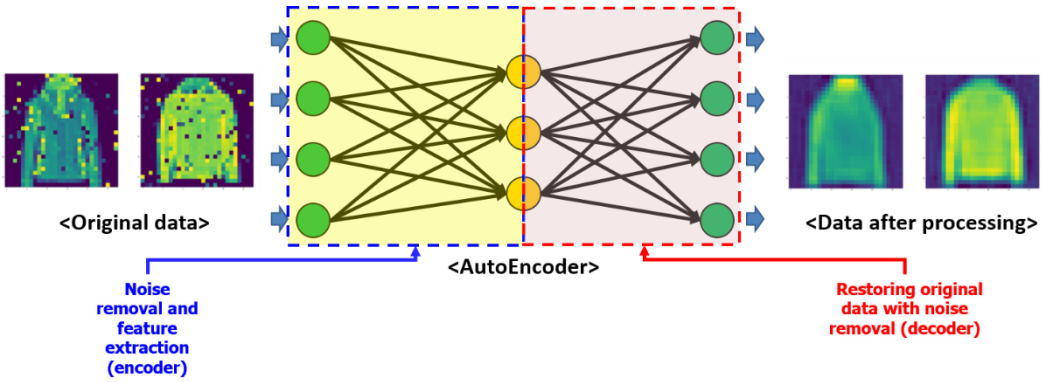

Figure 8. Configuration of AutoEncoder

In this study, an AutoEncoder was added in front of the convolutional LSTM to predict ocean environmental data grasping the noise-removed ocean environmental data's time-series characteristics. Figure 9 shows the configuration of the prediction model with AutoEncoder. First, the imaged ocean environmental data is input to AutoEncoder. After that, the data passed through the AutoEncoder is input to the convolutional LSTM.

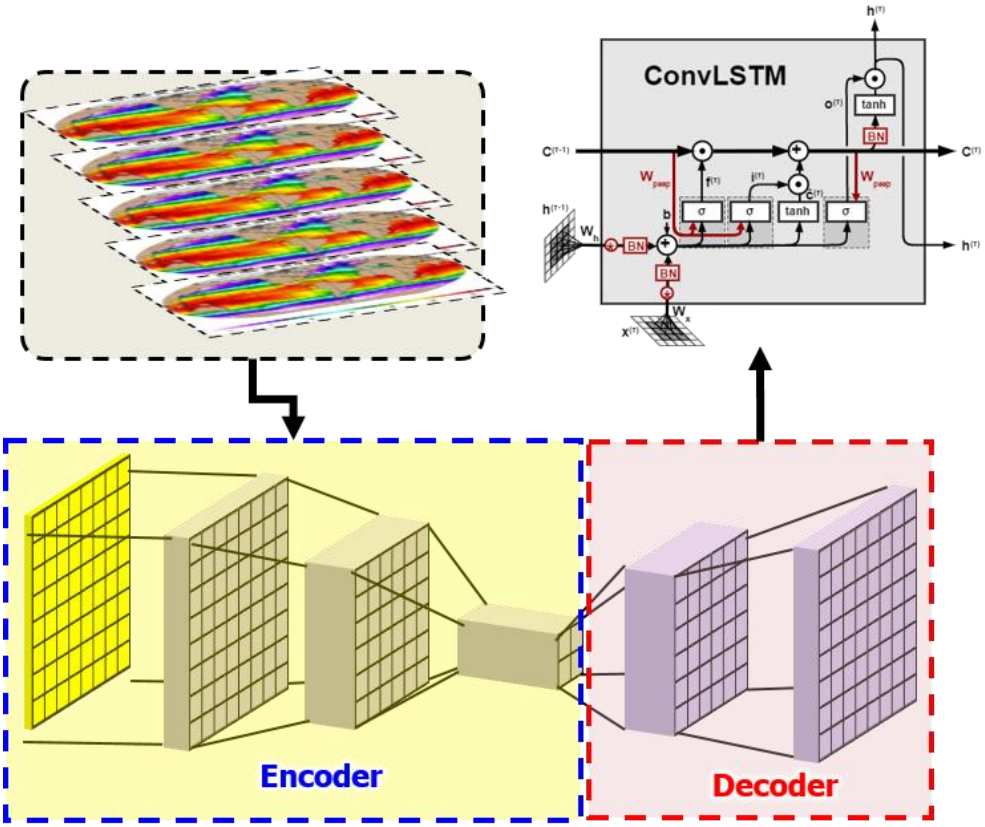

Figure 9. Configuration of a prediction model with AutoEncoder

3. Prediction method of ship power

In this study, we propose a prediction model of ship power based on DFN, a type of deep learning that effectively predicts numerical data. For training the prediction model of ship power, six types of ocean environmental data (SST, wave height, wave period, wave direction, wind speed, wind direction), three types of ship operational data (ship speed, ship draft, ship power), ship power data was used. Several methods were used to improve the prediction accuracy. Firstly, pre-processing of ocean environmental data was performed. (Figure 10-1) Secondly, the structure of DFN was changed in consideration of the data characteristics.(Figure 10-2) Finally, hyperparameters optimization (Figure 10-3) and K-means clustering (Figure 10-4) were performed. This section introduces the process from pre-processing of ocean environmental data to the hyperparameters optimization and K-means clustering. Figure 10 shows the entire process of prediction of ship power.

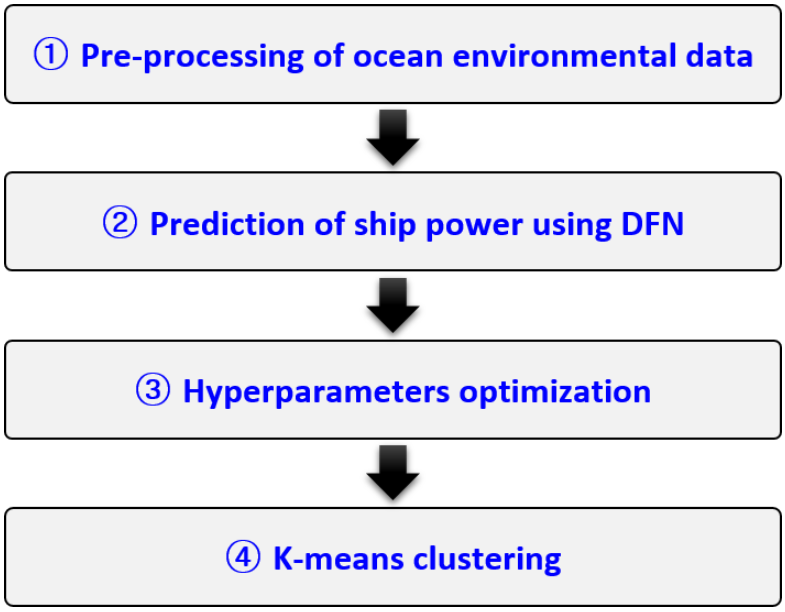

Figure 10. The entire process of ship power prediction

3.1. Pre-processing of ocean environmental data

The ocean environmental data related to wind and wave need to be applied differently. This is because the degree of application of ocean environmental data is different between the ship's stationary state and the operating state. Therefore, in this study, the ocean environmental data were converted to relative values to the ship's velocity. The wave height and wave period used in this study were derived from the wave spectrum. Since the wave spectrum changes when the ship moves, it must be converted to the ship's speed. The Equation is shown in Equation (13)-(14).

$$w_e = \left| w - \left(\frac{w^2 U_0}{g} \right) \cos \mu_0 \right| \tag{13}$$

$$S_\varsigma(w_e) = S_\varsigma(w) / \left| 1 - (\frac{2wU_0}{g}) \cos \mu_0 \right| \tag{14}$$

In Equations (13)-(14), μ_0 is an angle between ship and wave, U_0 is ship velocity, w_e is an encounter frequency, $S_\varsigma(w)$ is existing wave spectrum, and $S_\varsigma(w_e)$ is the converted wave spectrum considering ship velocity, respectively. The Equation of calculating wave height (SWH) and wave period (MWP) in the converted wave spectrum is shown in Equations (15)-(16).

$$m_{nj} = \int_0^\infty w^n S_j(w) dw \tag{15}$$

$$H_{1/3} = 4\sqrt{m_{oj}} \tag{16}$$

$$T = 2\pi \sqrt{\frac{m_{0j}}{m_{2j}}} \tag{17}$$

In Equations (15)-(17), $H_{1/3}$ is the significant wave height, T is the mean wave period, and m is the moment of the wave spectrum. In this study, $H_{1/3}$and T were defined as the pre-processed wave height and wave period and used to predict the ship's required power. Figure 11 shows the process of pre-processing of wave height and wave period.

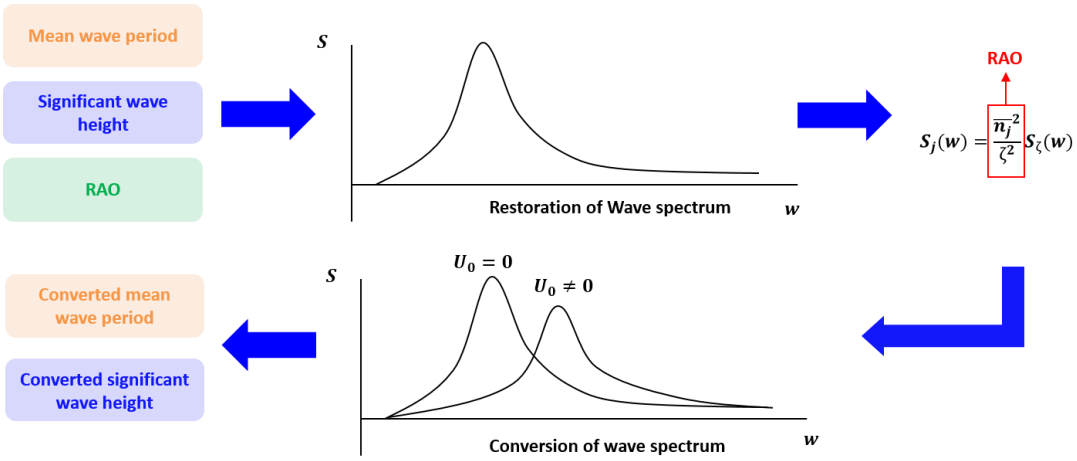

Figure 11. Process of pre-processing of wave height and wave period

3.2. DFN for ship power prediction

Among various deep learning models, DFN is mainly used for predicting numerical data. Since the prediction of the ship's required power can be viewed as a numerical data problem, in this study, the ship's required power was predicted using DFN. DFN is composed of an input layer, a hidden layer, and an output layer. In general, ocean environmental data and ship;s operational data are mainly used to predict a ship's required power (Liang et al., 2019). Therefore, in this study, the input layer was constructed using ship operational data and ocean environmental data, and the ground truth, which is a prediction target, was constructed using the ship's required power. In order to independently consider ocean environmental data and ship's operational data, model 2, which is different from the general DFN configuration, was developed. This was compared

with the general DFN model (DFN1). Figure 12 shows the structure of DFN (DFN1) used in this study. All data are inputted in one input layer.

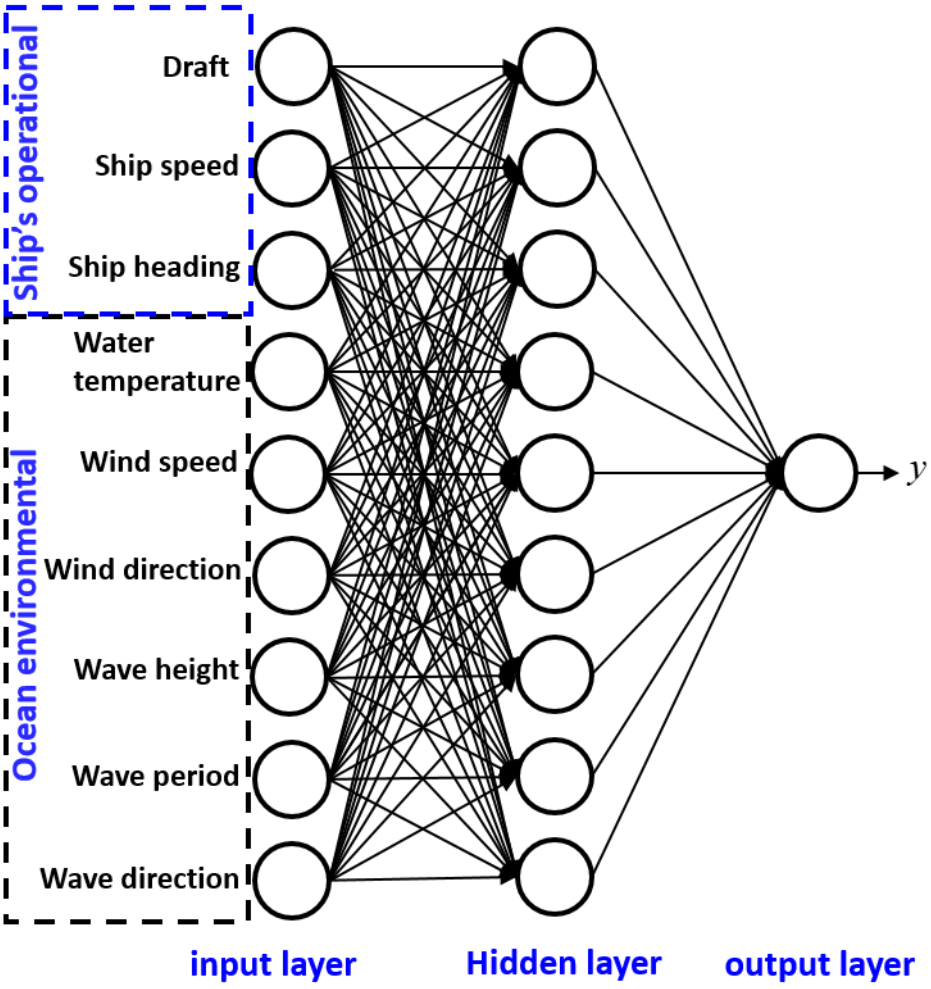

Figure 12. Structure of DFN1

Figure 13 shows the structure of DFN2. Two types of data (ocean environmental data,

ship’s operational data) are independently inputted to the input layer.

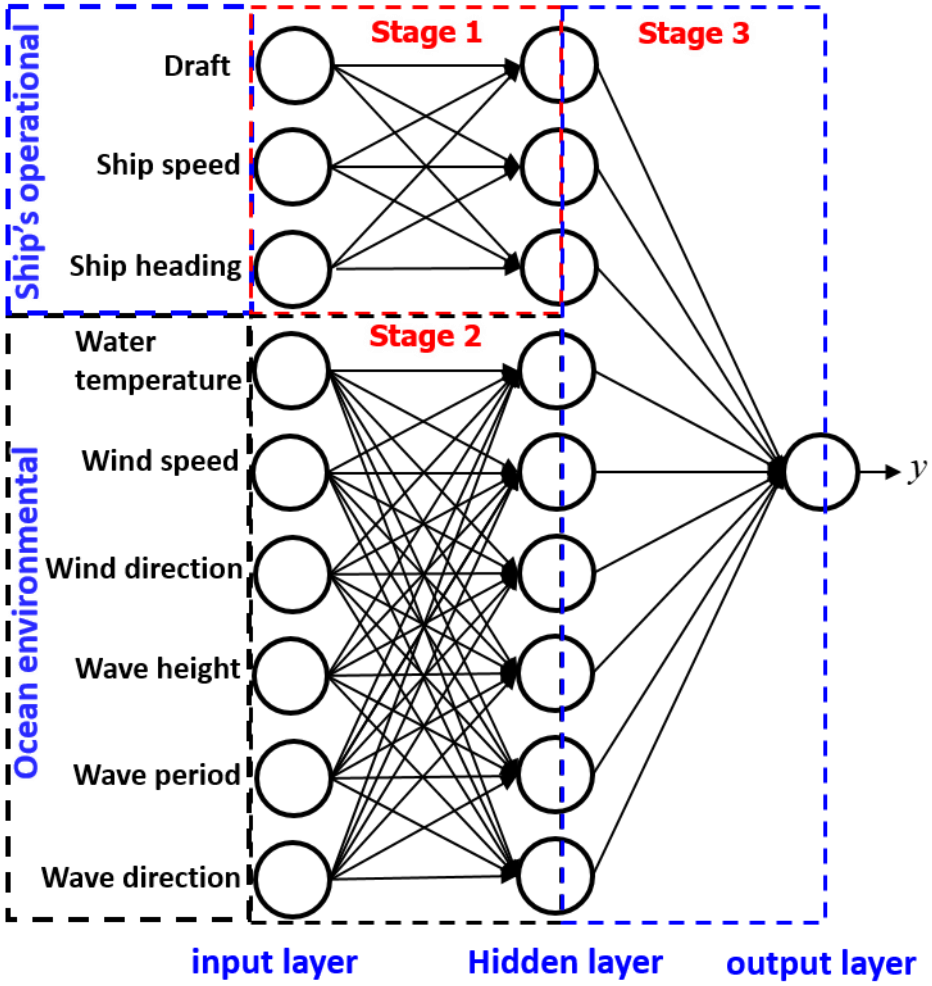

Figure 13. Structure of DFN2

The prediction performance of DFN is greatly affected by hyperparameter. Therefore, in this study, optimization was performed for five hyperparameters that have a great

influence on the prediction performance. Figure 14 shows five types of hyperparameters used for optimization in this study.

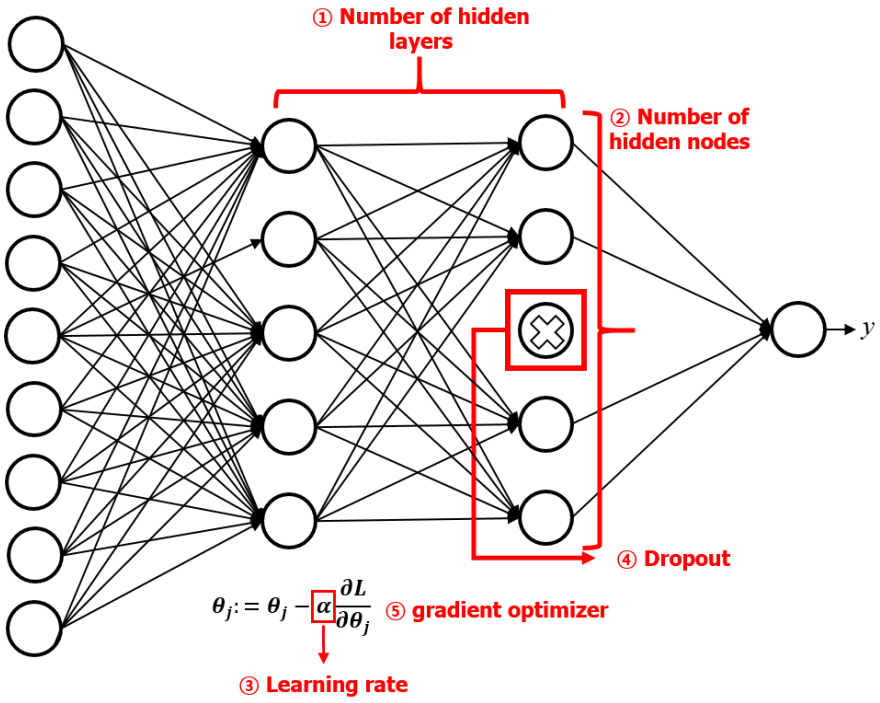

Figure 14. Hyperparameters of DFN

Firstly, the number of hidden layers (Figure 14-1) and hidden nodes (Figure 14-2) requires tuning according to the complexity of the problem. In general, the more complex the problem is, the more features to be expressed, so this hyperparameter should be high. However, if this hyperparameter is too high, overfitting may occur, so adjustment is necessary. Next, the learning rate (Figure 14-3) is a hyperparameter that indicates the

degree of weight update. If the learning rate is too high, the optimal solution cannot be found well. If the learning rate is too low, it takes a long time to learn and may fall into the local minimum, which also requires appropriate adjustment. Next, dropout (Figure 14-4) (Hinton et al., 2012) is a method of limiting nodes participating in learning to prevent overfitting. Dropout is known to have a great effect on regularization (prevent overfitting). However, since there are many types of models to be trained, it takes a long time to learn. Finally, it is a type of gradient optimizer (Figure 14-5). Gradient optimizer is a method of updating weights during training, and accordingly, there is a big difference in learning performance. In this study, three gradient optimizers were utilized: Stochastic Gradient Descent (SGD) (Bottou and Bousquet, 2009), Root Mean Square Propagation (RMSprop) (Ruder, 2016), and ADAM (Adaptive Moment Estimation) (Kingma and Ba, 2015). SGD is a traditionally used optimizer, and RMSprop and ADAM are designed to prevent falling into the local minimum, taking into account the inertia of the previous weight. The gradient optimizer also makes a big difference in learning performance.

In general, two methods are widely used for the optimization of these hyperparameters. First, the grid search method evaluates the performance of all hyperparameter combinations and selects the hyperparameter that shows the best performance among them. The random search method evaluates the performance of random hyperparameter combinations and selects the hyperparameter that shows the best performance among them. Although it is known that the random search method searches more efficiently than the grid search method, the grid search method, which evaluates the performance of all combinations, was used. Figure 15 shows the grid search method. This method evaluates the performance of the specified hyperparameter.

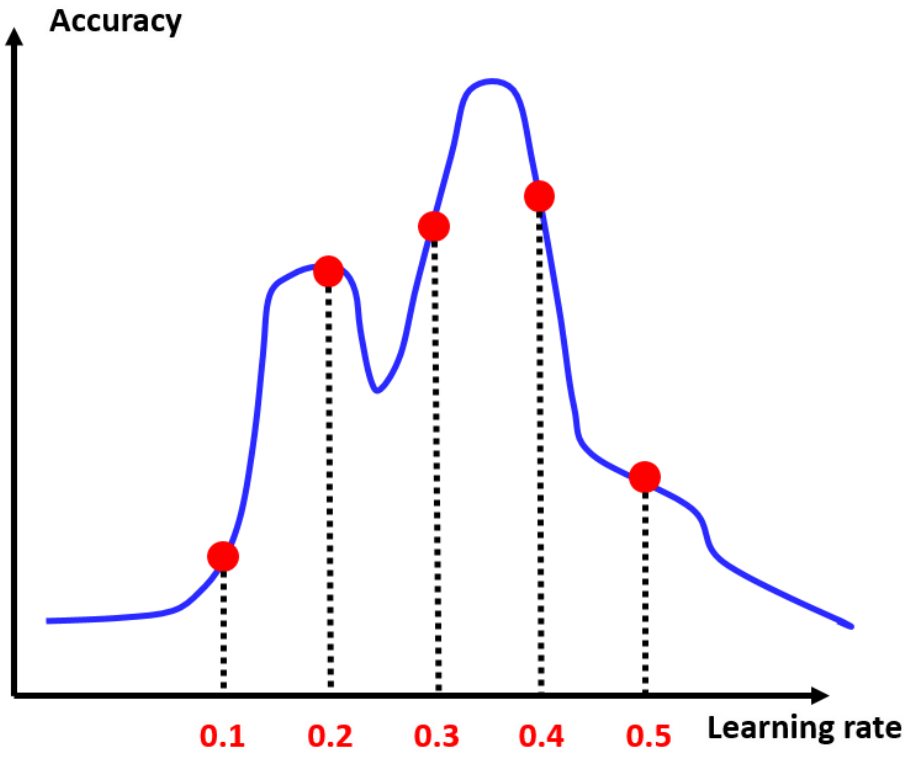

Figure 15. Grid search method

3.3. k-means clustering

The ship's required power is greatly affected by the sea state and the ship's operational condition. Therefore, in this study, it was determined that an independent prediction model was needed. For this, k-means clustering (Lloyd, 1982), which is mainly used for data clustering, was used. k-means clustering is a type of unsupervised learning. When the

number of clusters and the criteria for clustering is determined, clustering is performed autonomously. k-means clustering uses Equation (18) as an objective function to judge whether clustering is successful.

$$J = \sum_{n=1}^{k} \sum_{x_i \in c_n} \left\| x_i - u_n \right\|^2 \tag{18}$$

In Equation (18), u_n means the centroid of the nth cluster, and x_i means data belonging to each cluster. As shown in Equation (18), k-means clustering is the process of finding the cluster that minimizes the objective function and the center point of the cluster. Looking at the detailed process, first, the center point of the initial cluster is determined. After that, the data is clustered according to the center point. After that, we redefine the center point for each cluster according to the objective function. Finally, clustering is performed again for the newly defined center point. Continue the above process until the objective function converges. Figure 16 shows the process of k-means clustering.

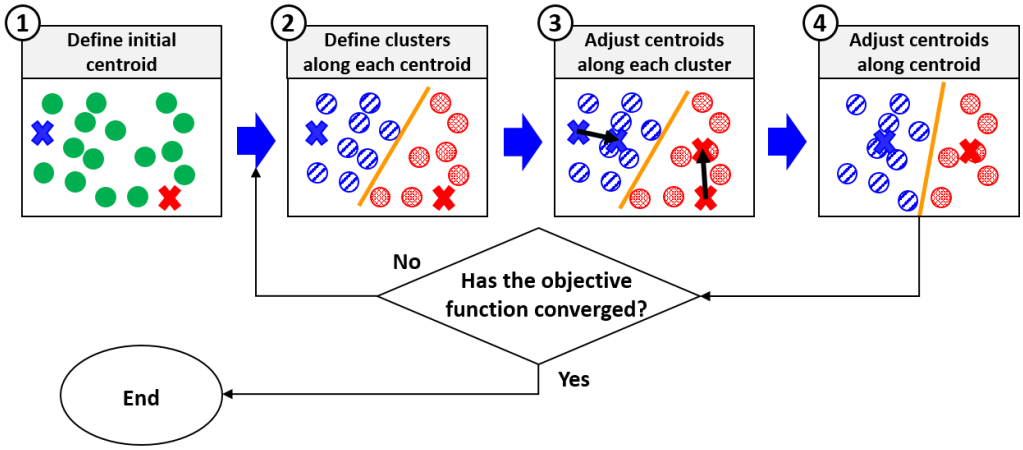

Figure 16. Process of k-means clustering

4. Verification

4.1. Verification of the prediction model of ocean environmental data

To verify the prediction model of ocean environmental data, the results were compared with the prediction results of other papers. P.Jain et al. (Jain and Deo, 2008) used the previous wave height and DFN to predict the wave height after 24 hours (prediction period: 2000.01.01 ~ 2000.08.28). Figure 17 shows the structure of DFN used in the study of P.Jain et al. (2008).

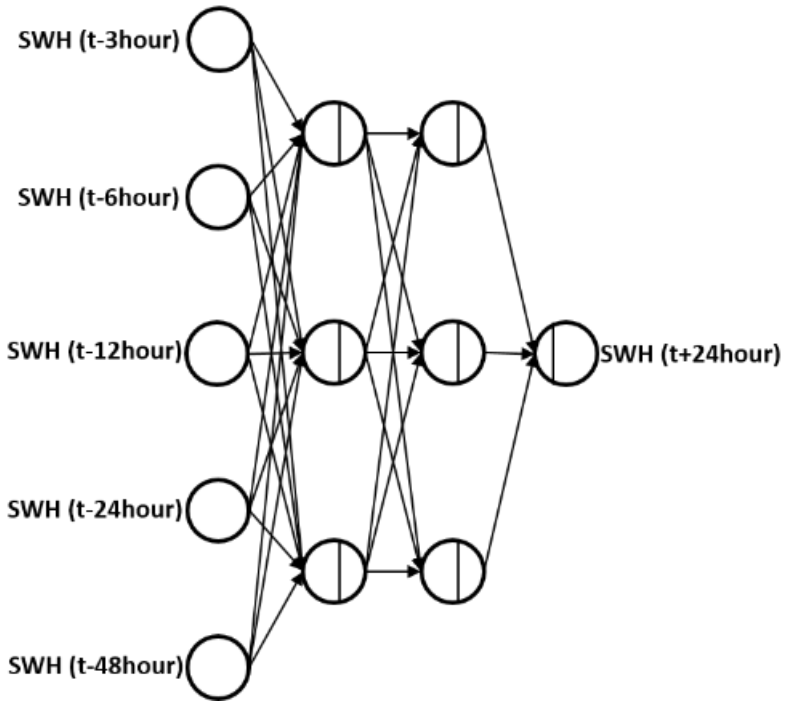

Figure 17. Structure of DFN (Jain and Deo, 2008)

In this study, the prediction results of this study and the prediction results of the convolutional LSTM used in this study were compared. Figure 18 shows the prediction result of this study and the study of P.Jain et al. (2008).

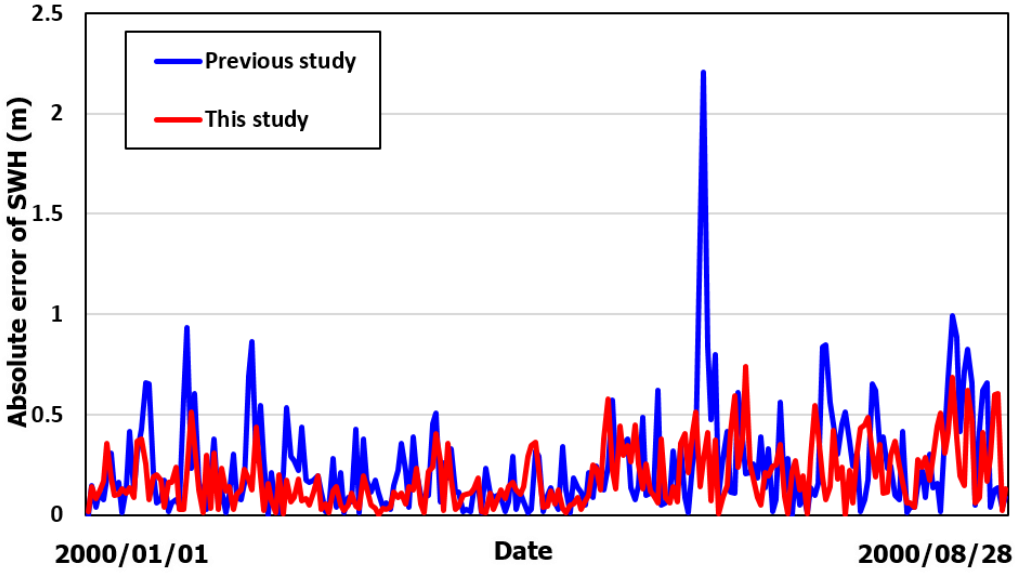

Figure 18. The comparison result of wave height

The mean absolute error (MAE) of the previous study was 0.245 m (5.5%), and the MAE of the convolutional LSTM was 0.188 m (5.0%). Compared to previous studies, it showed better prediction accuracy, and through this, it was confirmed that convolutional LSTM makes more accurate predictions than the conventional method using DFN.

For additional verification, the accuracy of the prediction method used by the weather forecasting center was compared. In ECMWF, the root mean square error (RMSE) was calculated according to the prediction period for the wave height and wind speed. This was compared with the prediction accuracy of convolutional LSTM. Figure 16 is a comparison of the prediction accuracy of the prediction method used in this study and the weather forecasting center for SWH based on RMSE.

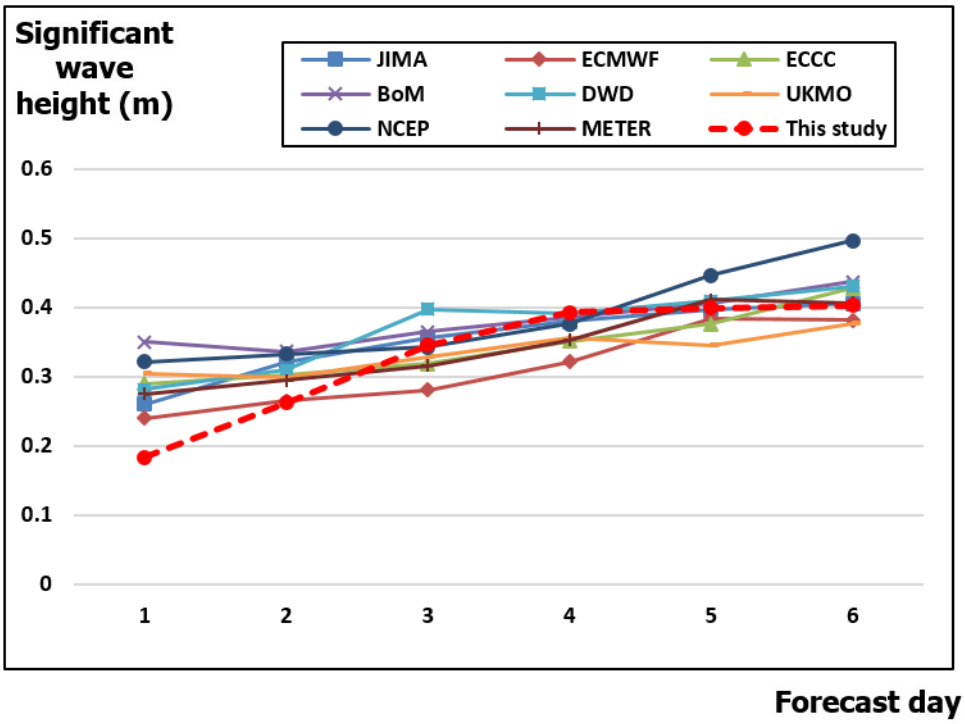

Figure 19. Comparison of RMSE with other prediction methods (SWH)

Looking at the RMSE of significant wave height (SWH), it was confirmed that the error gradually increased as the prediction period increased. The RMSE of the convolutional LSTM increased from 0.18m to 0.4m. Figure 20 is a comparison of the prediction accuracy of the prediction method used in this study and the weather forecasting center for wind speed based on RMSE.

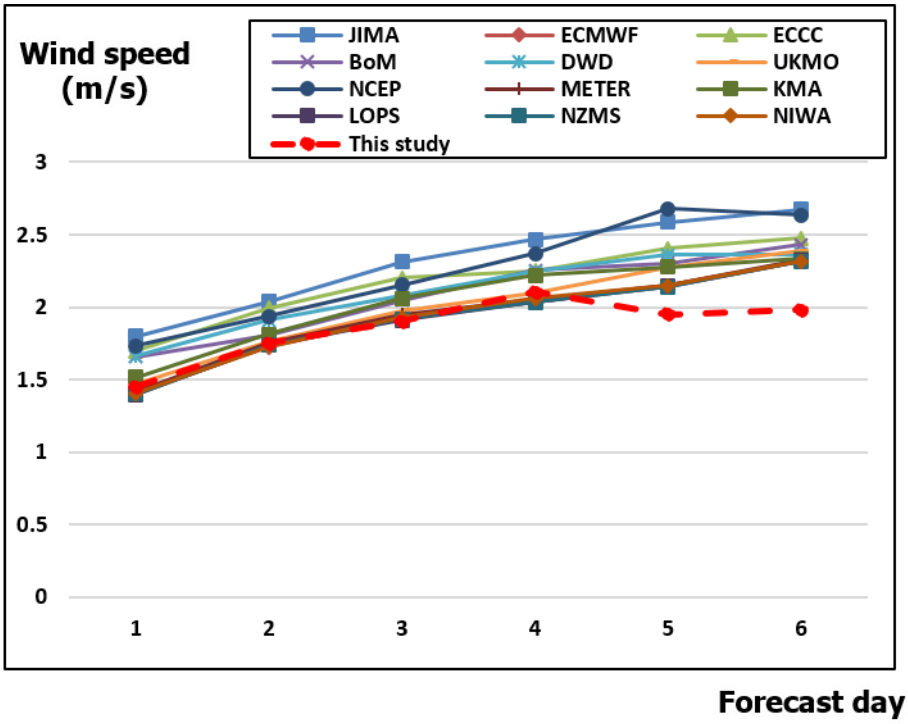

Figure 20. Comparison of RMSE with other prediction methods (wind speed)

Looking at the RMSE of wind speed, it was confirmed that the error gradually increased as the prediction period increased. The RMSE of convolutional LSTM increased from 1.45m/s to 2.1m/s. Based on these results, it was confirmed that the accuracy of the prediction model proposed in this study was not significantly different from the method used in the weather forecasting center.

4.2. Verification of the prediction model of ship power

Since it is difficult to obtain actual data on the 13,000 TEU-class container ship, which is the target of the prediction of the ship's required power, in this study, the prediction model was trained using the ship's required power based on the ISO 15016 method. To verify this, the prediction results were compared for 4,600 TEU-class ships that can generate data similar to the actual. The gray box model (GBM) ("Samsung Heavy Industries Energy efficiency management system," 2016) developed by Samsung Heavy Industries (SHI) shows an error of 0.4% from the actual ship's required power so that it can be assumed as actual data. Ocean environmental data and ship's operational data were used as input to GBM, and the ship's speed, ship's power, and fuel oil consumption (FOC) were calculated through this. Figure 20 shows the prediction process of the ship's required power using GBM.

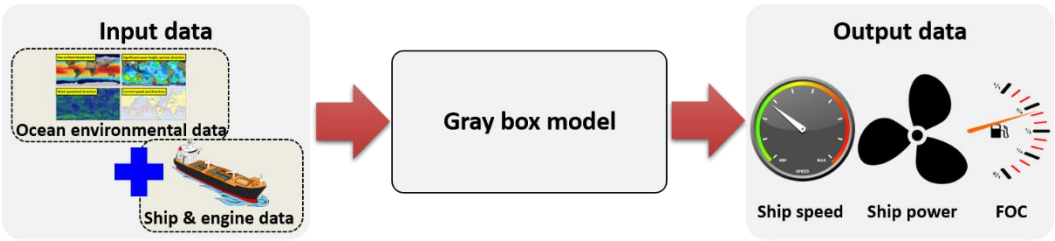

Figure 21. Ship power prediction using the GBM (Kim and Roh, 2020)

In this study, a DFN prediction model was created using the ship's required power generated based on the ISO 15016 method for comparison with the ship's required power using GBM. Table 3 shows hyperparameters for the DFN model.

Table 3. Hyperparameters for DFN model

Number of hidden layers	Number of hidden nodes	Learning rate	Dropout	Gradient optimizer
5	40	0.001	0	Adam

Table 4 shows the comparison of the prediction result of ship power.

Table 4. comparison of the prediction result of ship power

Comparison target	Output data	MAE (%)
Ship's power of ISO	Ship's power of DFN	370 KW (5.16%)
Ship's power of GBM	Ship's power of DFN	445KW (6.19%)

When comparing the ship's required power of ISO and the ship's required power of DFN, the average error is about 370KW (5.16%), and when comparing the ship's required power of DFN and Ship's required power of GBM, the average error is about 445KW (6.19%). Through this, it was confirmed that the error of DFN is 1.03% higher than that of the actual data, and it was confirmed that DFN could be used to predict the actual data of the ship.

5. Applications

5.1. Prediction result of ocean environmental data

Various methods were used in this study to find the optimal model for predicting ocean environmental data. First, prediction of ocean environmental data for the North Sea was carried out to confirm whether prediction using LSTM was possible. By inputting 8 years of past ocean environmental data into LSTM, prediction models for SST, SWH, MWP, wind speed-u, wind speed-v, current speed-u, and current speed-v were developed and trained. AutoEncoder was applied to solve the delay prediction problem, and convolutional LSTM, which extends LSTM, was used for predicting the ocean environmental data in all seas. The ocean environmental data of the past 20 years were used. The ocean environmental data for the entire sea area could not be trained at once due to memory problems, so the entire sea area was divided into 12 areas. Also, a total of 36 models were used for the prediction of the entire sea area by using three prediction models for each area.

5.1.1. Prediction for a single area

Figure 22 shows the configuration of the data set. First, a data set was constructed for training the prediction model. In ECMWF, data for a total of 8 years were used, training using data from 6 years, verification using data from 1 year, and testing using data from 1 year. In HYCOM, data for a total of 4 years and 4 months were used, and the data for 4 years were used for training, 2 months data for verification, and 2 months data for testing. The data set consisted of one month's ocean environmental data as input data and 5 days later ocean environmental data as output data.

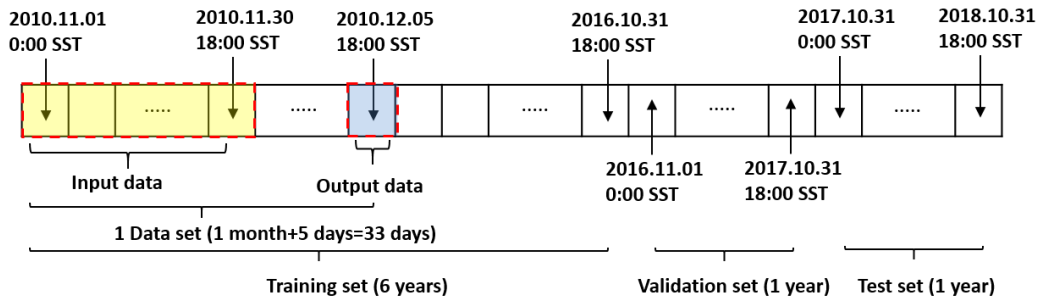

Figure 22. Configuration of the data set

In this study, LSTM was used to predict ocean environmental data. LSTM model can be classified into a many to one model and a many to many model according to the number of output data. In the many to one model, multiple data is input, and one data is output. In the many to many model, multiple data is input, and multiple data is output. Figure 23 shows the structure of many to one model. The loss function is calculated once because the number of output data is one.

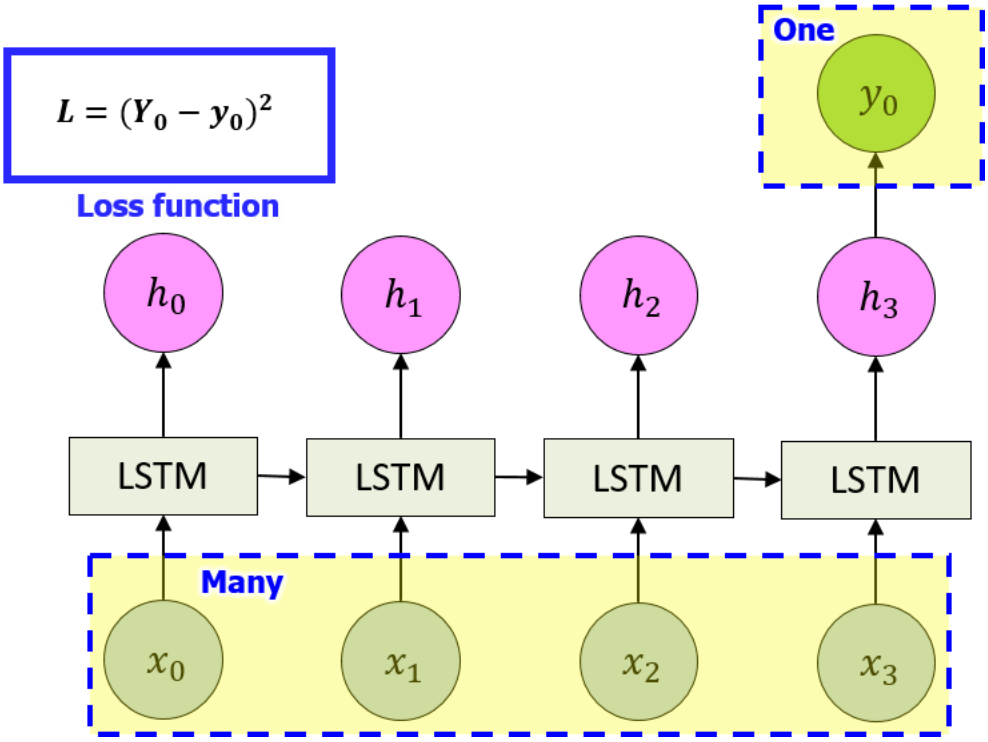

Figure 23. Structure of many to one model

Figure 24 shows the structure of many to many model. The loss function is calculated multiple times because there are multiple outputs.

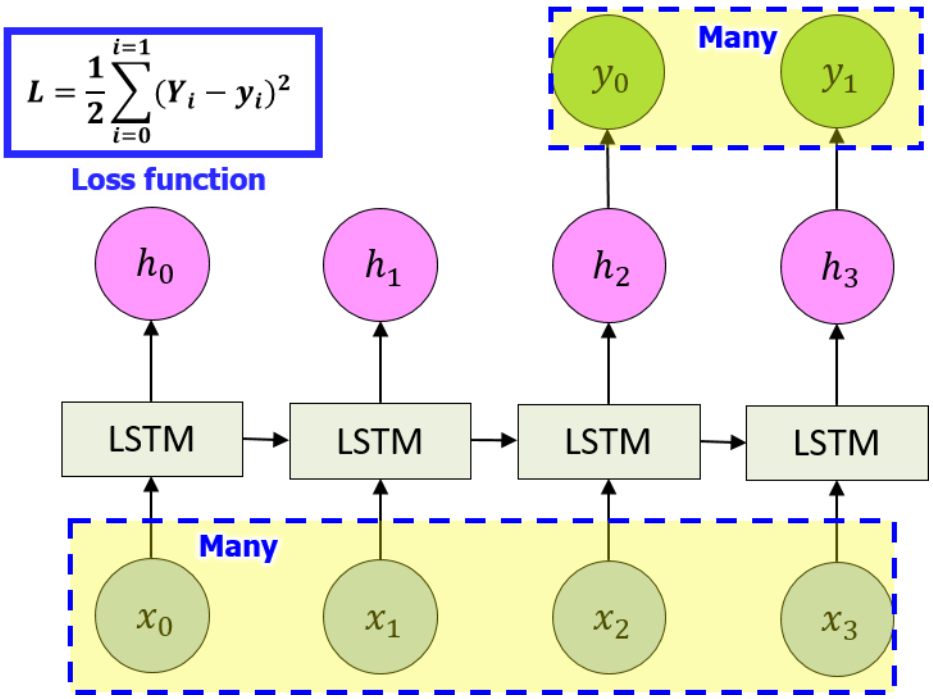

Figure 24. Structure of many to many model

When comparing the many to one model and the many to many model, it can be seen that the loss function differs accordingly because the output type is different. Table 5 shows the results of predicting ocean environmental data using many to one model and many to many model.

Table 5. Comparison of prediction result between many to one and many to many model

Prediction method	Input data	Number of input nodes	Output data	Number of output nodes	Number of nodes per hidden layer	MAE
Many to	SST	120	SST	1	32	0.474℃

one		(120 days)		(30 day)		(5.26%)
Many to many	SST	120 (120 days)	SST	1 (30 day)	32	0.484°C (5.37%)

When comparing the many to one model and the many to many model, there was no significant difference in prediction accuracy. To find out the predicted ocean environmental data according to the input data's length (look back range) and the prediction time (look forward range), the results were compared by changing the input data period and the prediction time. In the case of input data, we compared 3 cases of 1 month, 15 days, 7 5 days, and compared 3 cases of 1 day, three days, and five days in the case of prediction time. Table 6 shows the prediction results according to the input data period.

Table 6. Prediction result according to input data period

Prediction method	**Input data**	**Number of input nodes (look back range)**	**Output data**	**Number of output nodes (look forward range)**	**Number of nodes per hidden layer**	**MAE**
LSTM	SST	120 (30 days)	SST	1 (5 day)	16	0.306°C (4.34%)
LSTM	SST	60 (15 days)	SST	1 (5 day)	8	0.319°C (4.53%)
LSTM	SST	30 (7.5 days)	SST	1 (5 day)	16	0.328°C (4.66%)

Looking at the prediction results according to the look back range, it can be seen that the longer the lookback range, the better the result, and the other ocean environmental data also showed similar trends. Table 7 shows the prediction results according to the look forward range. Looking at the prediction results according to the look forward range, it can be seen that the shorter the look forward range, the better the result is, and other ocean

environmental data also shows a similar trend.

Table 7. Prediction result according to prediction time

Prediction method	**Input data**	**Number of input nodes (look back range)**	**Output data**	**Number of output nodes (look forward range)**	**Number of nodes per hidden layer**	**MAE**
LSTM	SST	120 (30 days)	SST	1 (5 day)	32	0.306°C (4.34%)
LSTM	SST	120 (30 days)	SST	1 (3 day)	32	0.255°C (3.62%)
LSTM	SST	120 (30 days)	SST	1 (1 day)	32	0.185°C (2.62%)

Table 8 shows the optimal prediction result of all ocean environmental data. In general, it was confirmed that the longer the lookback range and the shorter the look forward range, the better the prediction result was. In addition, it was found that most of the ocean environmental data were within 10% of the relative error.

Table 8.Optimal prediction result of all ocean environmental data

Prediction method	**Input data**	**Number of input nodes (look back range)**	**Output data**	**Number of output nodes (look forward range)**	**Number of nodes per hidden layer**	**MAE**
LSTM	SST	120 (30 days)	SST	1 (1 day)	32	0.19°C (2.7%)
LSTM	SWH	120 (30 days)	SWH	1 (1 day)	32	0.67m (7.2%)
LSTM	MWP	120 (30 days)	MWP	1 (1 day)	32	0.95s (10.8%)
LSTM	MWD	120	MWD	1	32	11.05°

		(30 days)		(1 day)		(2.63%)
LSTM	Current speed	240 (30 days)	Current speed	1 (1 day)	32	0.06m/s (17.5%)
LSTM	Current direction	240 (30 days)	Current direction	1 (1 day)	64	34.67° (9.63%)
LSTM	Wind speed	120 (30 days)	Wind speed	1 (1 day)	32	1.35m/s (10.6%)
LSTM	Wind direction	120 (30 days)	Wind direction	1 (5 day)	32	14.83° (4.1%)

5.1.2. Effects of AutoEncoder

AutoEncoder is applied to solve delayed prediction, which occurs when predicting time series data using LSTM. Figure 25 shows the prediction result using LSTM and AutoEncoder. Looking at the prediction results of LSTM model using AutoEncoder, it was confirmed that delayed prediction was significantly resolved.

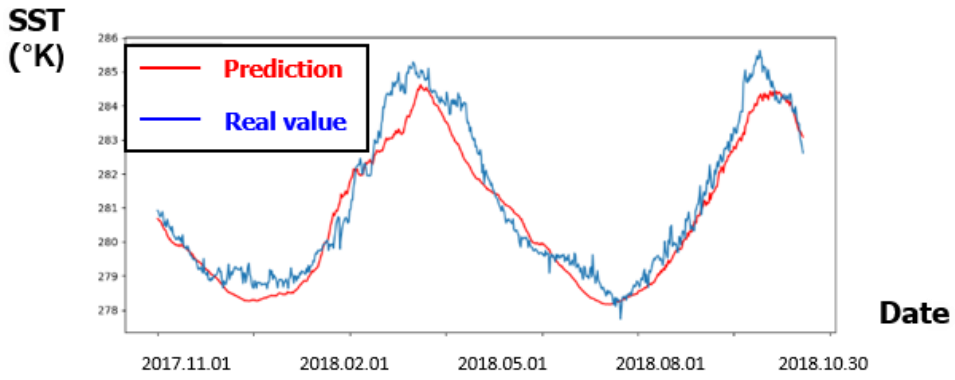

Figure 25. Prediction result using LSTM and AutoEncoder

Table 9 compares the prediction result using the AutoEncoder. As a result of comparing LSTM model with applying AutoEncoder and the general LSTM model, it was confirmed that the error was reduced by 53%. Through this, it was confirmed that AutoEncoder not only solved the delayed prediction but also improved the prediction accuracy.

Table 9. Comparison of prediction result using the AutoEncoder

Prediction method	**Input data**	**Number of input nodes (look back range)**	**Output data**	**Number of output nodes (look forward range)**	**Number of nodes per hidden layer**	**MAE**
LSTM (many to one)	SST	120 (120 days)	SST	1 (30 day)	32	0.988°C (10.97%)
AutoEncoder+LSTM (many to one)	SST	120 (120 days)	SST	1 (30 day)	32	0.474°C (5.26%)

5.1.3. Prediction for all sea areas

In order to confirm the effectiveness of the prediction using convolutional LSTM, ocean environmental data for the west coast were extracted, and the prediction results were confirmed using convolutional LSTM. The ocean environmental data of the sea area of the west coast of latitude 32°~36° and longitude 121°~125° were extracted and imaged. The image size is 4 (number of horizontal pixels) x 4 (number of vertical pixels). After inputting this image to AutoEncoder, the result was input to Convolutional LSTM to predict the

ocean environmental data of the sea area. A model that predicts ocean environmental data after 15 days was constructed by inputting 60 days of previous ocean environmental data and six kinds of data of ECMWF (water temperature, wave height, wave period, wave direction, wind speed in longitudinal direction –u, wind speed in latitude direction –v) was set to each channel. Table 10 shows the result of the prediction for the west coast. As a result of the prediction for the west coast, it was confirmed that the prediction of the sea area is possible using the Convolutional LSTM. In addition, it was possible to predict the entire ocean environmental data with one model without creating a model for each data. A test of prediction using convolutional LSTM on the west coast confirmed that prediction is possible. However, there were questions about the expansion of prediction for all sea areas. Therefore, the convolutional LSTM was trained for the sea area, including the actual ship's route, and the prediction accuracy of the model was compared.

Table 10. Result of prediction for the west coast

Prediction method	**Input data**	**Number of input nodes (look back range)**	**Output data**	**Number of output nodes (look forward range)**	**Number of nodes per hidden layer**	**MAE**
Convolutional LSTM	SST	240 (60 days)	SST	1 (15 day)	32	6.029°C (1.97%)
Convolutional LSTM	SWH	240 (60 days)	SWH	1 (15 day)	32	0.470m (5.67%)
Convolutional LSTM	MWP	240 (60 days)	MWP	1 (15 day)	32	2.130s (4.19%)
Convolutional LSTM	MWD	240 (60	MWD	1 (15 day)	32	67.084° (18.63%)

		days)				
Convolutional LSTM	Wind u10	240 (60 days)	Wind u10	1 (15 day)	32	2.859m/s (6.03%)
Convolutional LSTM	Wind v10	240 (60 days)	Wind v10	1 (15 day)	32	2.455m/s (7.43%)

Figure 26 shows the prediction results of the Mediterranean sea after 6 hours. Because it predicted for a short look forward range, it was confirmed that the overall prediction was accurate. However, it was not possible to accurately predict SST.

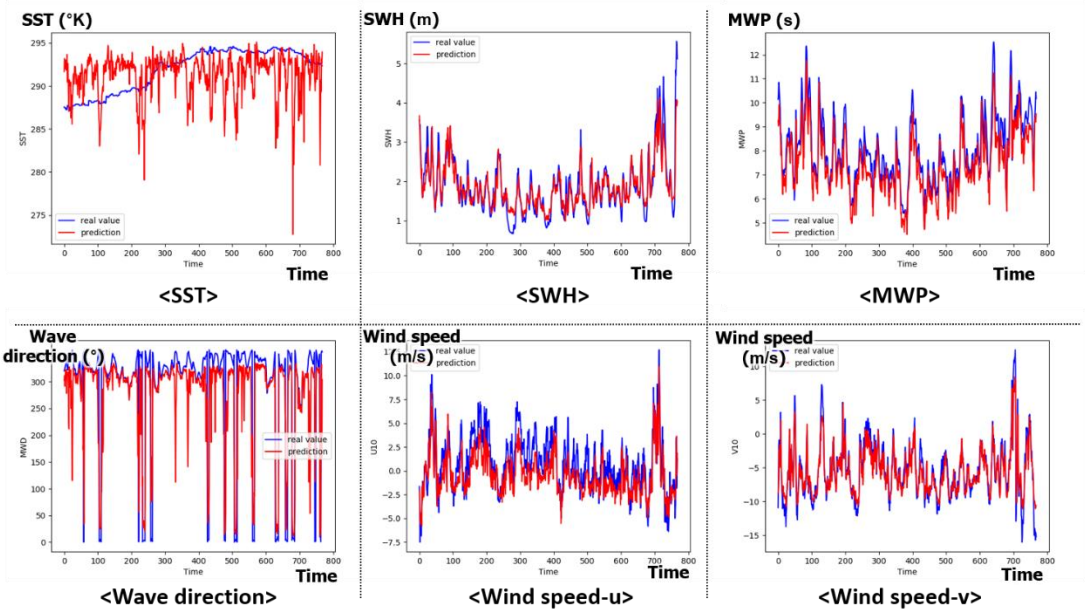

Figure 26. Prediction result of Mediterranean sea after 6 hours

Figure 21 shows the prediction result of the Mediterranean sea after one day. As the look forward range increased, it was confirmed that although the prediction was not more accurate than the sea weather prediction after 6 hours, it still predicted well.

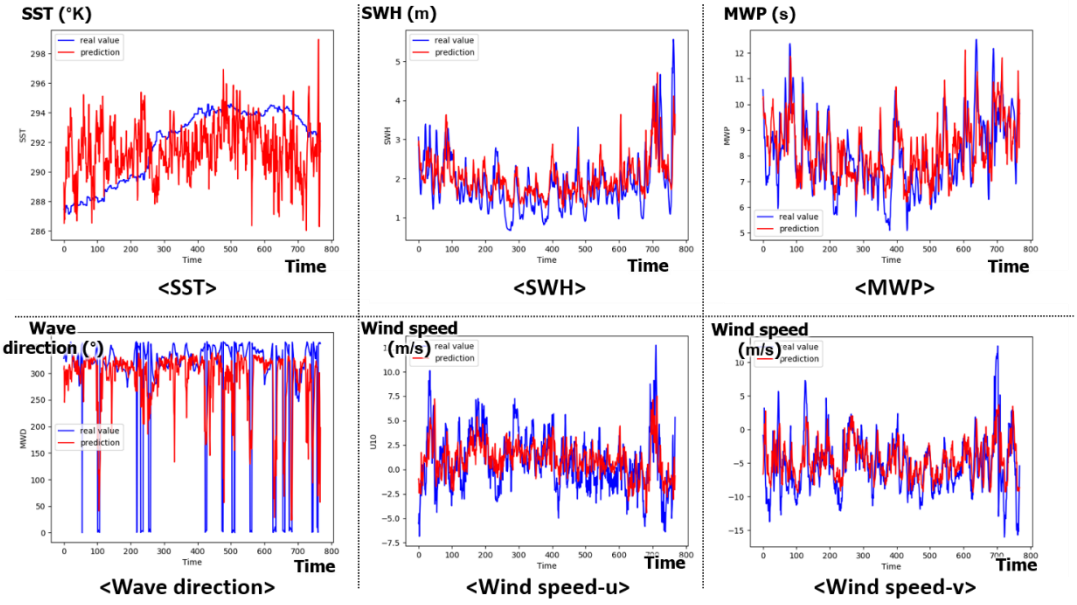

Figure 27. Prediction result of Mediterranean sea after 1 day

Figure 28 shows the prediction result of the Mediterranean sea after two days. Looking at the prediction results according to the look forward range, it was confirmed that the prediction accuracy decreased as the look forward range became longer, like LSTM.

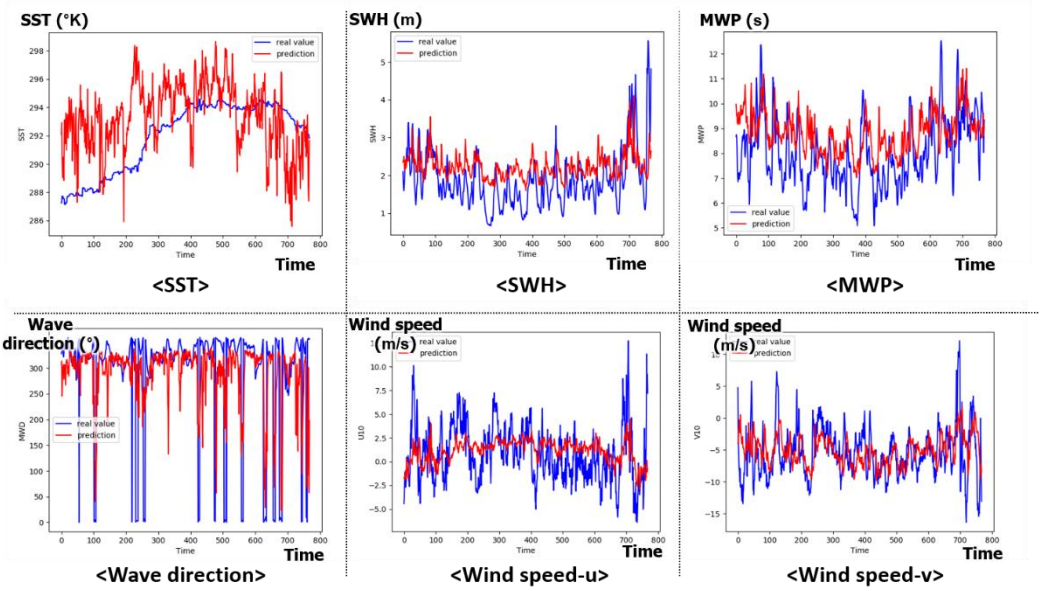

Figure 28. Prediction result of Mediterranean sea after 2 days

From LSTM test results, the longer the lookback range, the better the prediction result was, but because only 22.5 days of ocean environmental data were input due to memory problems, the accurate prediction was not made. In order to consider this problem, two cases were tested. The first is to train a model that predicts after one step (6 hours) that derives the most accurate prediction result and then accumulate it to predict data after several steps. The second is to change the time interval of data from 6 hours to 24 hours in order to input data for a long period of time, and input data for more periods to predict because data of several steps cannot be set as input data due to memory problems. After testing these two cases, they were compared with the existing prediction results. Figure 29 shows the process of accumulating prediction after training a model that predicts after one step.

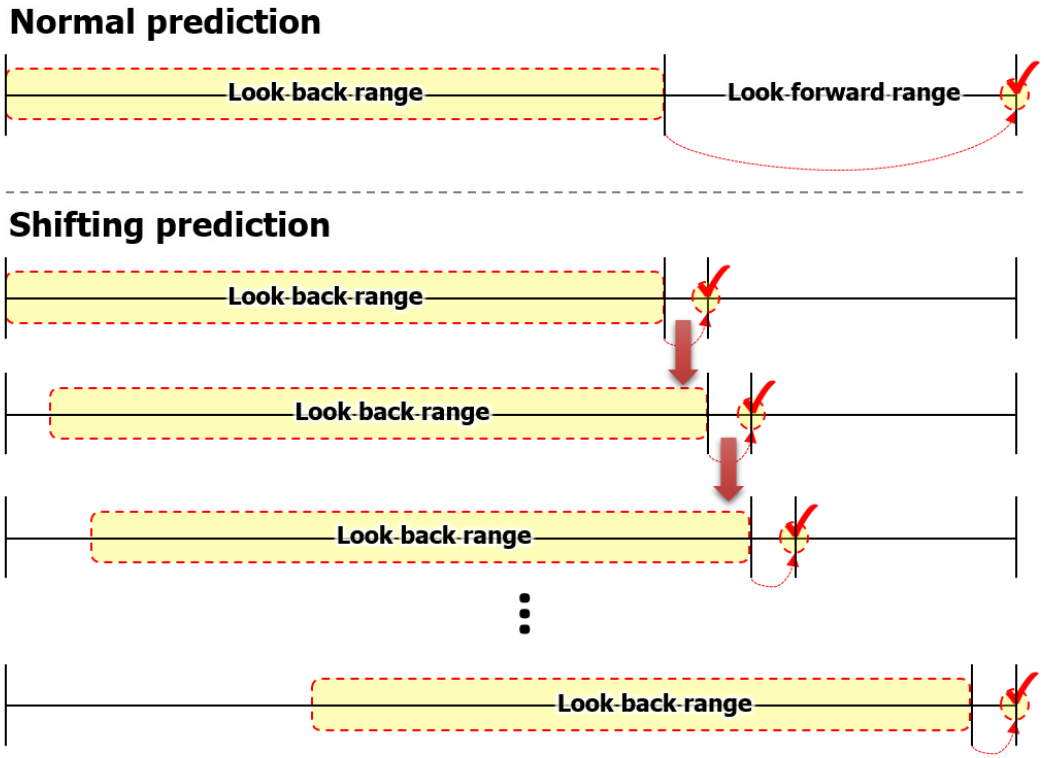

Figure 29. Process of shifting prediction

Figure 30 shows the learning process after changing the time interval of data from 6 hours to 24 hours.

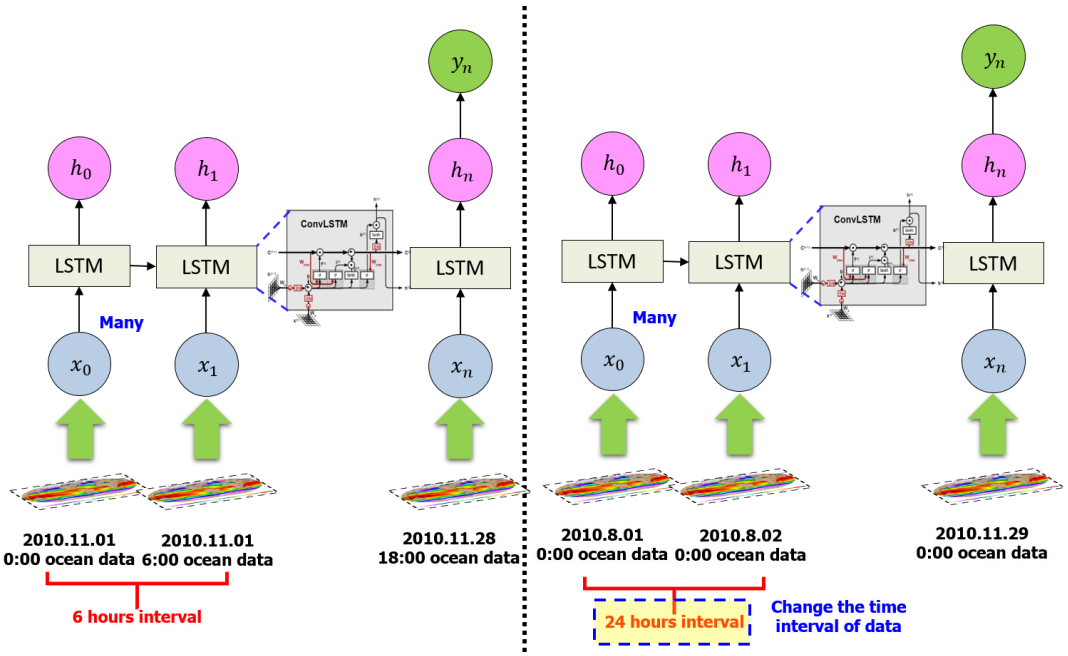

Figure 30. Process of changing interval of data

In this study, the prediction accuracy for various cases was derived from investigating the effects of look back range, look forward range, channel configuration, and shifting predicting. Table 11 shows the configuration of the prediction model.

Table 11. Configuration of the prediction model

Cases	**Input data range (look back range)**	**Output data (look forward range)**	**Channel configuration**
Case 1	60 days (240)	After 6 hours (1)	1 channel (SST)
Case 2		After 6 hours (1)	
Case 3		After 1day (4)	

Case 4	22.5 days (90)	After 2 days (8)	6 channels (SST, MWH, MWP, MWD, WU,WV)
Case 5		After 3 days (12)	
Case 6		After 7 days (28)	
Case 7		After 3 days (1-shifting)	
Case 8	90 days (90)	After 7 days (7)	
Case 9	84 days (84)	After 7 days (7)	1 channel (SST), 5 channels (MWH, MWP, MWD, WU, WV)

Figure 31 shows the result of shifting prediction after three days. As a result of shifting prediction, the prediction was not more accurate than the existing prediction method.

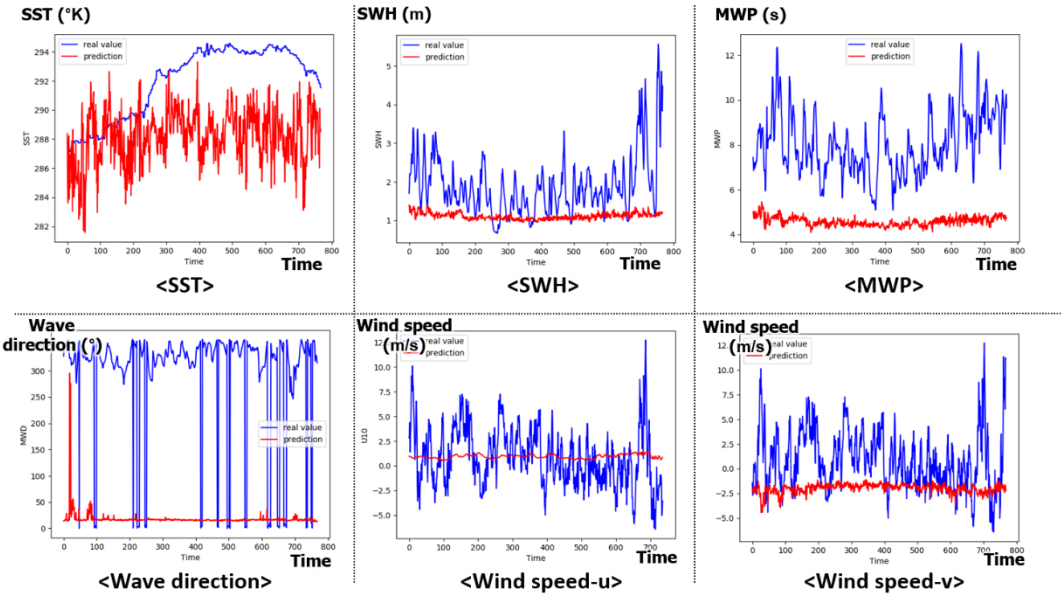

Figure 31. Result of shifting prediction after three days

Figure 32 shows the prediction result of changing time intervals of data after seven days. As a result of changing the time interval of data, there was no significant difference from the existing prediction method.

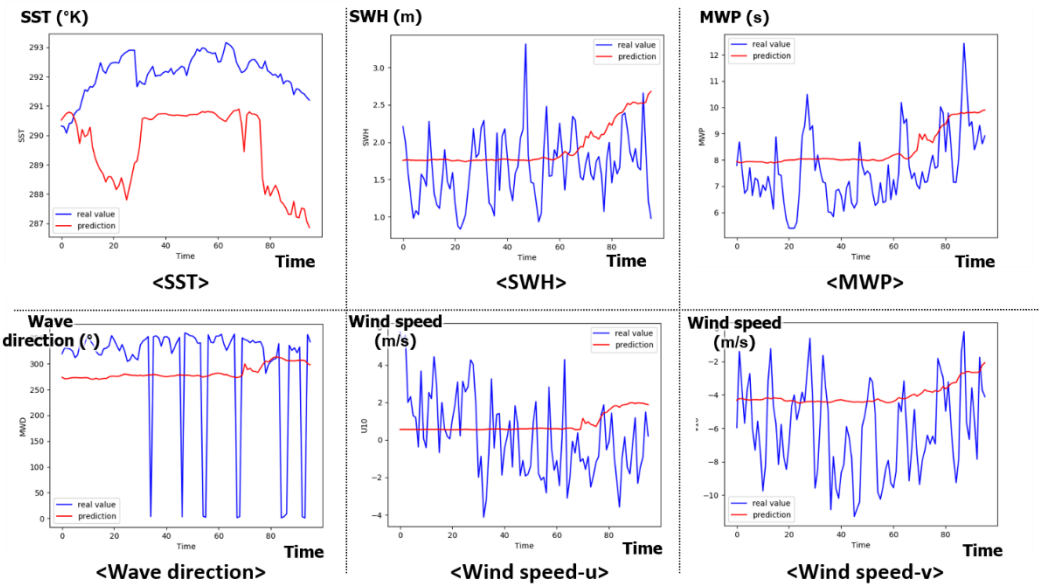

Figure 32. Prediction result of changing time interval of data after seven days

Table 12 shows the prediction result about several cases. As a result of the prediction, the method of prediction by accumulating one step has a very low accuracy compared to the existing prediction results. The method of prediction by changing the time interval of data was similar to the existing prediction result, or better results were derived in the case of wind speed. Also, in the case of water temperature, it was better to predict only water temperature data than to predict it with other ocean environmental data. In this study, we aimed to predict ocean environmental data for all sea areas. However, it is difficult to train

all the seas at once due to the limitation of the memory problem, so the seas excluding the polar regions (latitude -67.5°~67.5°, longitude 0°~360°) were divided into 12 divisions, and training was conducted for each area.

Table 12. Prediction result about several cases

Cases	**SST error [°K]**	**MWH error [m]**	**MWP error [s]**	**MWD error [deg]**	**WU error [m/s]**	**WV error [m/s]**	**Average error [%]**
Case 1	1.84 (9.3%)	N/A	N/A	N/A	N/A	N/A	9.3
Case 2	2.84 (9.3%)	0.09 (0.6%)	0.25 (1.4%)	11.21 (3.1%)	1.21 (2.0%)	1.19 (2.1%)	3.1
Case 3	3.31 (10.8%)	0.13 (0.8%)	0.32 (1.4%)	19.43 (5.3%)	1.80 (2.9%)	1.84 (3.2%)	4.1
Case 4	2.69 (8.8%)	0.18 (1.2%)	0.40 (2.3%)	28.34 (7.8%)	2.28 (3.7%)	2.24 (3.9%)	4.6
Case 5	3.68 (12.1%)	0.22 (1.5%)	0.48 (2.8%)	33.76 (9.3%)	2.46 (4.0%)	2.38 (4.1%)	5.6
Case 6	3.16 (10.4%)	0.18 (1.2%)	0.42 (2.4%)	32.15 (8.9%)	2.33 (3.8%)	2.24 (3.9%)	5.1
Case 7	7.03 (23.1%)	0.28 (1.8%)	0.95 (5.5%)	66.12 (18.3%)	3.41 (5.5%)	3.46 (5.6%)	10.0
Case 8	4.11 (13.5%)	0.17 (1.4%)	0.44 (2.5%)	32.66 (9.0%)	2.05 (3.4%)	1.99 (3.8%)	5.6
Case 9	3.47 (4.2%)	0.44 (3.5%)	0.75 (4.7%)	28.27 (7.8%)	3.06 (5.0%)	3.17 (5.2%)	5.1

Figure 33 shows the result of dividing the entire sea area into 12 areas.

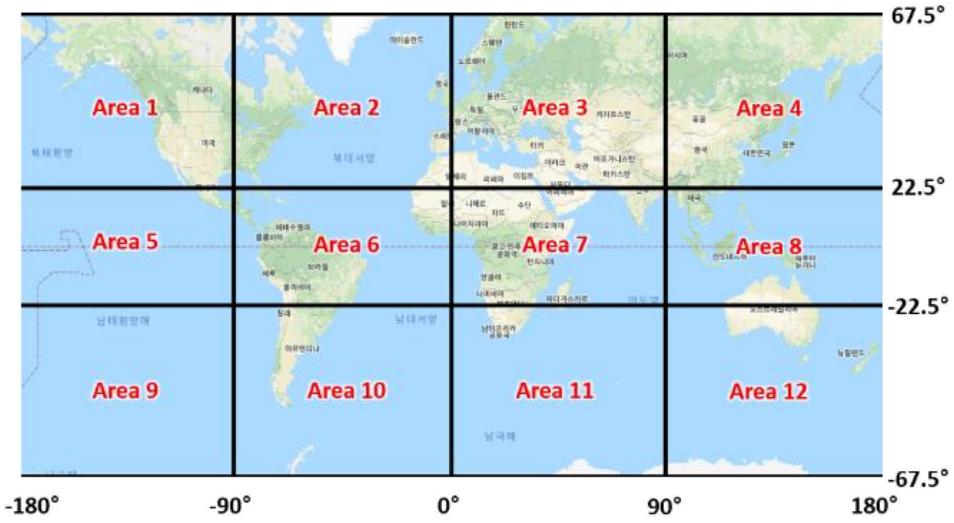

Figure 33. All sea area divided into 12 areas

Figure 34 shows the prediction result of area 2. It can be seen that the wave-related data is well predicted.

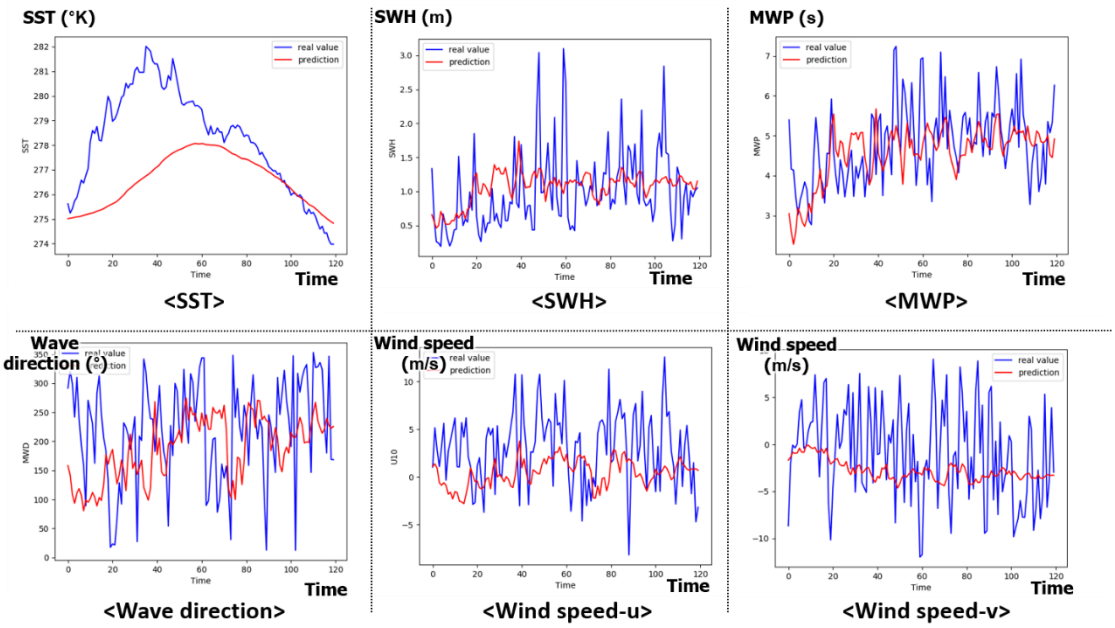

Figure 34. Prediction result of area 2

Figure 35 shows the prediction result of area 3. Overall, no accurate predictions were made.

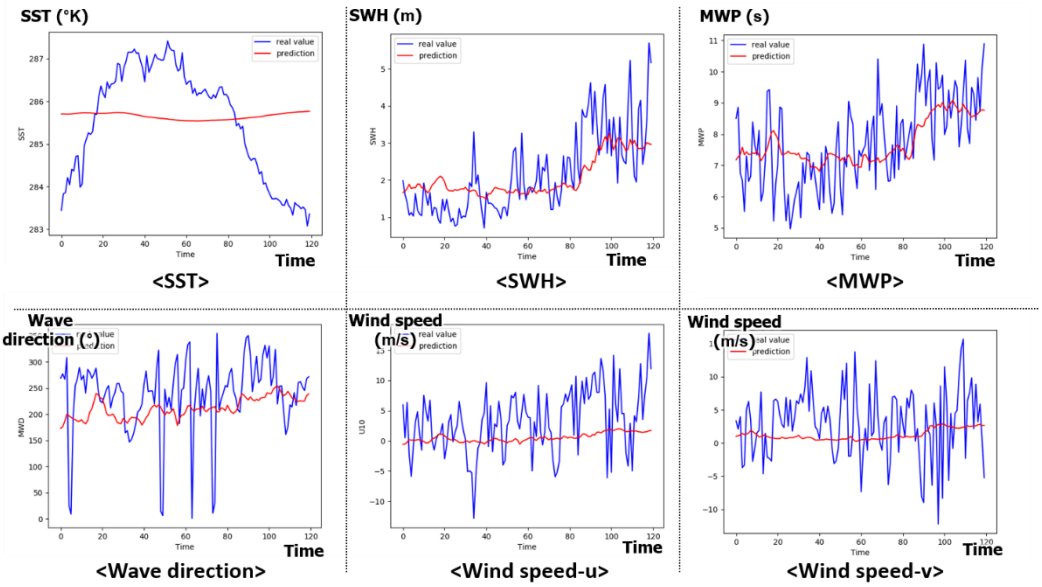

Figure 35. Prediction result of area 3

Table 13 shows the prediction result of all sea areas. As a result of training ocean environmental data for all sea areas, it was confirmed that all ocean environmental data except wave direction were predicted within 10% of relative error. Looking at the prediction results for each sea area, the prediction error for area 8 is small, and the prediction error for area 10 is large. In addition, when looking at the prediction results for each data, the relative error of the current speed was small, which is believed to be because the current has distinct seasonal characteristics, making it easy to identify patterns.

Table 13. Prediction result of all sea areas

Areas	SST error [°K]	MWH error [m]	MWP error [s]	MWD error [deg]	WU error [m/s]	WV error [m/s]	CU error [m/s]	CV error [m/s]	Average error

Area 1	2.81 (7.8%)	0.82 (5.1%)	1.15 (6.4%)	57.20 (15.9%)	4.04 (5.5%)	4.64 (5.9%)	0.12 (4.0%)	0.12 (3.7%)	6.8%
Area 2	2.05 (5.2%)	0.74 (4.4%)	1.10 (6.4%)	72.77 (20.2%)	6.01 (4.0%)	4.49 (4.3%)	**0.12 (2.5%)**	**0.11 (2.3%)**	6.2%
Area 3	3.74 (9.7%)	0.46 (3.7%)	**0.88 (5.3%)**	71.84 (20.0%)	3.56 (5.7%)	3.76 (6.4%)	0.09 (3.0%)	0.09 (3.0%)	7.1%
Area 4	3.47 (9.9%)	0.74 (4.6%)	1.07 (6.1%)	77.08 (21.4%)	20.18 (7.9%)	4.56 (3.6%)	0.15 (3.5%)	0.15 (3.1%)	7.5%
Area 5	3.70 (9.8%)	0.36 (4.6%)	1.13 (6.8%)	52.25 (14.5%)	**2.03 (4.1%)**	2.22 (3.6%)	0.13 (2.9%)	0.12 (3.2%)	6.2%
Area 6	**3.40 (9.9%)**	0.82 (5.5%)	**1.84 (11.0%)**	72.42 (20.1%)	3.33 (4.9%)	3.03 (4.9%)	0.14 (3.7%)	0.13 (3.5%)	7.9%
Area 7	1.63 (4.6%)	0.58 (6.2%)	1.42 (8.4%)	39.11 (10.9%)	3.54 (7.3%)	3.75 (6.5%)	0.15 (3.0%)	0.14 (3.0%)	6.2%
Area 8	**1.08 (3.0%)**	**0.34 (3.1%)**	0.82 (4.8%)	**29.29 (8.1%)**	2.21 (4.2%)	**2.00 (3.2%)**	0.13 (3.0%)	0.12 (3.1%)	**4.1%**
Area 9	1.34 (4.0%)	0.85 (6.0%)	1.17 (7.0%)	43.32 (12.0%)	**4.80 (8.0%)**	5.00 (7.8%)	**0.12 (4.1%)**	**0.12 (4.2%)**	6.6%
Area 10	2.38 (8.9%)	**1.09 (11.6%)**	1.76 (10.7%)	**77.47 (21.5%)**	5.47 (10.3%)	5.21 (9.1%)	0.13 (2.9%)	0.13 (2.9%)	**9.7%**
Area 11	2.92 (9.2%)	0.93 (6.2%)	1.36 (8.0%)	37.68 (10.5%)	5.00 (7.6%)	**7.96 (9.9%)**	0.15 (3.0%)	0.15 (2.6%)	7.1%
Area 12	1.07 (3.1%)	0.81 (5.4%)	1.10 (6.5%)	31.40 (8.7%)	4.52 (6.9%)	4.71 (6.3%)	0.13 (2.9%)	0.13 (3.1%)	5.4%
Average error	2.47 (7.1%)	0.71 (5.5%)	1.23 (7.3%)	55.15 (15.3%)	5.39 (6.4%)	4.28 (6.0%)	0.13 (3.2%)	0.13 (3.2%)	6.7%

5.2. Prediction result of ship power

The prediction model of the ship's required power was trained using datasheets for 72 13,000 TEU-class ships. The input data is composed of 3 types of data related to the ship's draft, ship speed, and heading of the ship, and 6 types of sea data such as water temperature, wind speed, wind direction, wave height, wave period, and wave direction. In the case of ground truth, the brake horsepower was set in consideration of the sea state. In the datasheet, data that does not match the actual ship operation situation, such as when the required

horsepower is abnormally large (ship power>64000KW), the ship's speed is abnormally large (ship speed>30kn), or the heading of the ship exceeds 360 degrees Excluded from training. Through this process, a total of 240,000 data sets were used for training. To verify the validity of the prediction model, the data set was divided into a train set, a validation set, and a test set. The train set is a data set for learning, and a total of 80% of data is used. A validation set is a data set to evaluate the performance of the model according to hyperparameters, and a total of 10% of data was used. The test set is data for evaluating the final performance of the model, and a total of 10% of the data was used. In addition, since the range of all data is different, min-max scaling was performed to convert data between 0 and 1.

5.2.1. Hyperparameters optimization

In this study, hyperparameters optimization was performed to select the optimal model for predicting the horsepower required of the ship. A total of 5 hyperparameters were optimized, and the tuning set of each hyperparameter was selected through trial and error methods. Table 14 shows the tuning set for hyperparameters optimization.

Table 14. Hyperparameters set for optimization

Hyperparameters	**Tuning set**
Number of hidden layers	3,4, 5, 6, 7
Number of hidden nodes	10, 20, 30, 40
Learning rate	0.0001, 0.001, 0.01
Dropout	0, 0.25, 0.5
Gradient optimization	ADAM, SGD, RMSProp

The performance evaluation of the predictive model was based on the average validation loss. The mean validation loss was calculated using mean square error (MSE), which is mainly used for model evaluation. Figure 36 shows the validation loss according to the number of hidden layers.

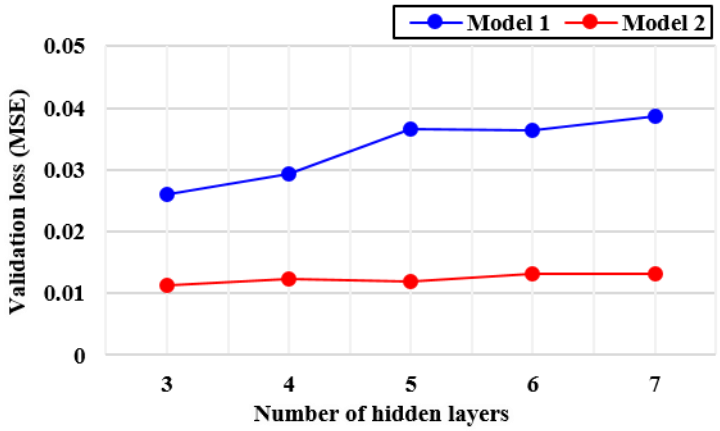

Figure 36. Validation loss according to number of hidden layers

It was confirmed that validation loss increased as the number of hidden layers increased. If the number of hidden layers is excessively increased, it is judged that unnecessary features increase, and accurate prediction cannot be made. Figure 37 shows the validation loss according to the number of hidden nodes.

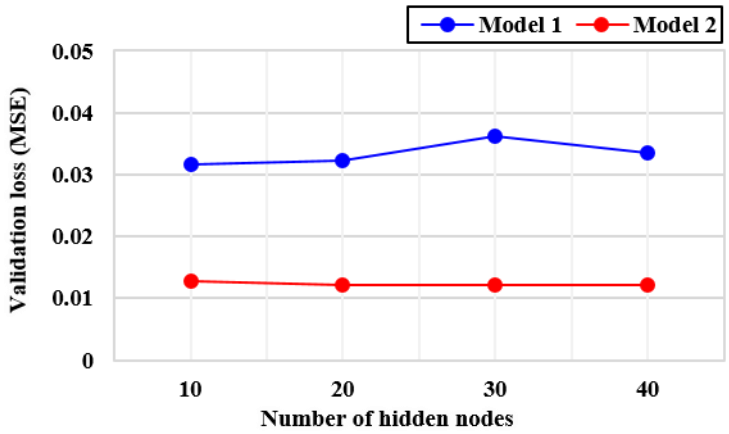

Figure 37. Validation loss according to number of hidden nodes

The number of hidden nodes did not show any significant pattern. Through this, it was confirmed that the number of hidden nodes did not significantly affect the prediction accuracy than the number of hidden layers. Figure 38 shows the validation loss according to the learning rate.

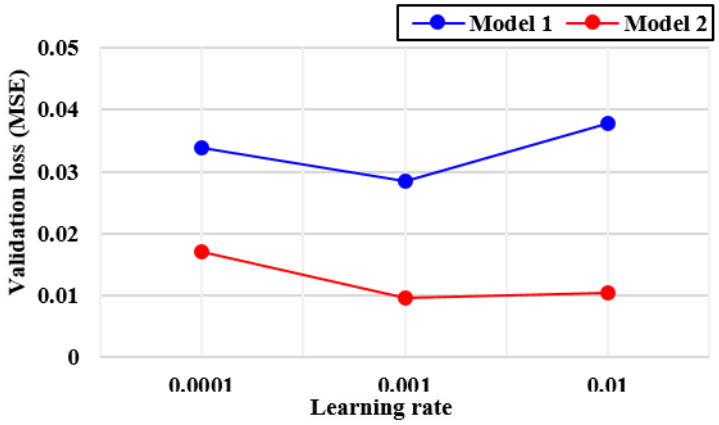

Figure 38. Validation loss according to the learning rate

When looking at the validation loss according to the learning rate, it was confirmed that the best result was obtained when the learning rate was 0.001. If the learning rate is too large, an optimal solution cannot be found, and if the learning rate is too low, the local minimum falls. Figure 39 shows validation loss according to dropout.

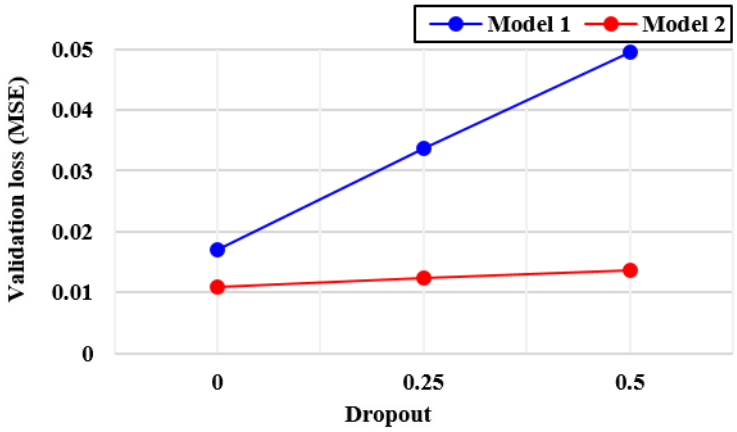

Figure 39. Validation loss according to dropout

The trend of validation loss according to dropout showed the best prediction accuracy when dropout was not used. In general, dropout is known to be effective in regularization to prevent overfitting, but it is judged to be ineffective in predicting the ship's required power. Figure 40 shows the validation loss according to the gradient optimizer.

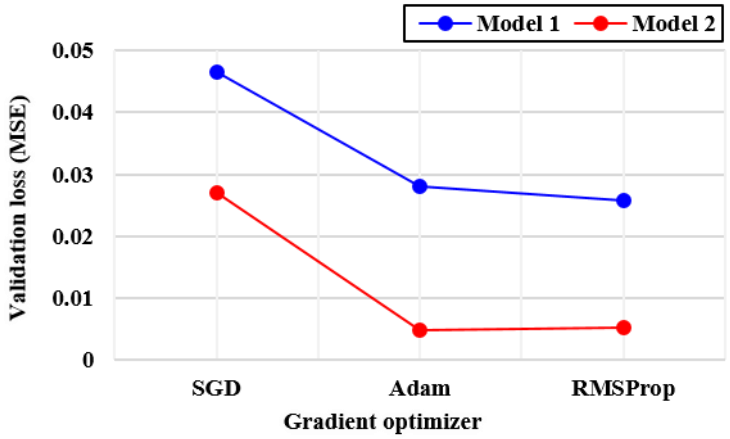

Figure 40. Validation loss according to gradient optimizer

The trend of validation loss according to gradient optimizer showed the best prediction accuracy when Adam and RMSProp were used. Through this, it was confirmed that Adam and RMSProp, designed to escape the local minimum, make better predictions than the traditionally used SGD. Looking at the overall hyperparameters optimization result, it can be seen that model 2 shows better prediction accuracy than model 1. This is considered to be because model 2 has fewer times to fall into the local minimum than model 1. In this study, as shown in Table 14, the performance of the model was evaluated for all 540 cases of hyperparameter combinations (5x4x3x3x3), and the hyperparameter combination showing the best prediction result was extracted. Table 15 shows the optimal hyperparameter combinations for model 1 and model 2. In the case of gradient optimizer, dropout, and learning rate, the optimal combination was derived when 0.001, 0, and RMSprop were selected as in the previous result.

Table 15. Result of hyperparameters optimization about model 1 and model 2

Model	Number of hidden layers	Number of hidden nodes	Learning rate	Dropout	Gradient optimizer
DFN (model 1)	6	40	0.001	0	RMSProp
DFN (model 2)	4	40	0.001	0	RMSProp

Figure 41 shows the prediction of model 1 using optimal hyperparameters. The estimation ratio was defined as the predicted value divided by the actual value. It was confirmed that the estimation ratio of most of the prediction data was formed around 1, and through this, it was confirmed that a reasonable prediction was made.

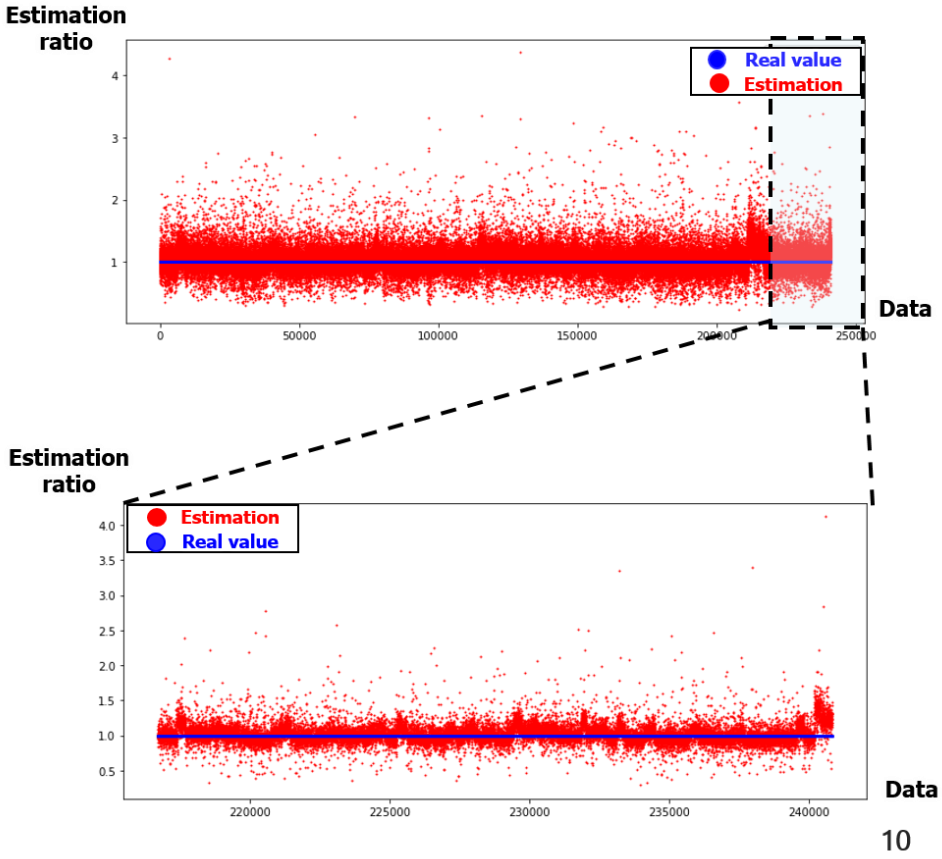

Figure 41. Prediction result of model 1 using optimal hyperparameters

5.2.2. Comparison with other prediction methods

To check whether DFN makes accurate predictions compared to commonly known numerical prediction methods, it was compared with multi-linear regression (MLR) (Draper and H.Smith, 1998) and support vector regression (SVR) (Vapnik, 2000), which are widely used. MLR is the most widely used method for numerical prediction and predicts results with a linear combination of independent variables. SVR is a regression method

based on a support vector machine (SVM). Table 16 compares with other prediction methods.

Table 16. Comparison with other prediction methods

Prediction method	**Pre-processing**	**MAE (%)**
MLR	X	2,749 KW (5.11%)
MLR	O	2,706 KW (5.03%)
SVR	X	2,326 KW (4.32%)
SVR	O	2,338 KW (4.34%)
DFN (model 1)	X	1,951 KW (3.62%)
DFN (model 1)	O	1,949 KW (3.62%)
DFN (model 2)	X	1,895 KW (3.52%)
DFN (model 2)	O	1,883 KW (3.50%)

When comparing the prediction results using DFN with the prediction results using MLR and SVR, the prediction accuracy decreased by 823KW (1.52%) and 443KW (0.82%). Through this, it was confirmed that DFN makes more accurate predictions than existing prediction methods. In addition, when comparing the prediction results of model 1 and model 2, the prediction accuracy decreased by 61KW (0.11%) when model 2 was used. Through this, it was confirmed that model 2 is a more advanced model.

5.2.3. Effects of K-means clustering

The ship's required power is greatly influenced by ship operational conditions and sea state. Therefore, in this study, K-means clustering was conducted for ship draft, ship speed, and Beaufort scale (wind speed) reflecting this. Table 17 shows the results of K-means clustering when the K value is set to 3.

Table 17. Clustering result of K-means clustering (K=3)

Clustering criteria	**Cluster 1**	**Cluster 2**	**Cluster 3**
Beaufort scale	0 ~ 4	5 ~ 7	8 ~ 12
Ship speed (knots)	0.1 ~ 12.3	12.4 ~ 18.0	18.1 ~ 29.7
Ship draft (m)	5.3 ~ 9.3	9.4 ~ 13.3	13.4 ~ 21.1

Looking at the results, it can be confirmed that clustering is properly performed. In this study, the accuracy of each prediction model was compared and analyzed by setting the K value to 3, 4, 5, and 6. Table 18 shows the prediction accuracy according to the K value and clustering criteria.

Table 18. Prediction result along with clusters

Number of clusters	**Clustering criteria**	**MAE (%)**
3	Beaufort scale	1,918 KW (3.56%)
4	Beaufort scale	1,966 KW (3.65%)
5	Beaufort scale	1,968 KW (3.66%)
6	Beaufort scale	1,965 KW

		(3.65%)
3	Ship speed	1,932 KW (3.59%)
4	Ship speed	1,900 KW (3.53%)
5	Ship speed	1,924 KW (3.57%)
6	Ship speed	1,973 KW (3.66%)
3	Ship draft	1,869 KW (3.47%)
4	Ship draft	1,898 KW (3.52%)
5	Ship draft	1,939 KW (3.60%)
6	Ship draft	1,890 KW (3.51%)

Looking at the prediction accuracy, it was confirmed that the prediction accuracy decreased when the number of clusters increased. It is believed that this is because an excessive increase in clusters decreases the number of train data in each cluster, and thus an accurate prediction model for each cluster cannot be derived. When K-means clustering was carried out, the best result was when it was divided into 3 clusters based on ship draft, and the error was 1,869KW (3.47%). When K-means clustering was not performed, the best prediction result was 1,8883KW (3.50%) using model 2, which is not much different from when K-means clustering was performed.

5.3. Development of a program for the prediction of ship power and ocean environmental data

Based on the previously developed prediction model of ocean environmental data and ship's required power, a program was developed to predict ocean environmental data and ship's required power when a ship's operating route is given. When a user defines a route, it predicts the ocean environmental data for the sea area that fits the defined route and predicts the ship's required power through it.

5.3.1. Configuration of the program's execution environment

The program was developed in .Net environment and python, and the deep learning model was developed through python, the internal software logic was developed in C# language, and the GUI was developed in XMAL language. The GUI was developed in the Windows Presentation Foundation (WPF) environment, and it was configured to smoothly interwork with the internal logic, external Python prediction model, and big data server. External APIs are not included for program development, and python libraries such as NumPy and Keras, and libraries for GUI configuration such as fluent. Ribbon, BingMap, Math.Net, and AvalonDock are utilized for deep learning models, internal logic, and GUI of the program.

5.3.2. The internal composition of the program

Figure 42 shows the internal composition of the program.

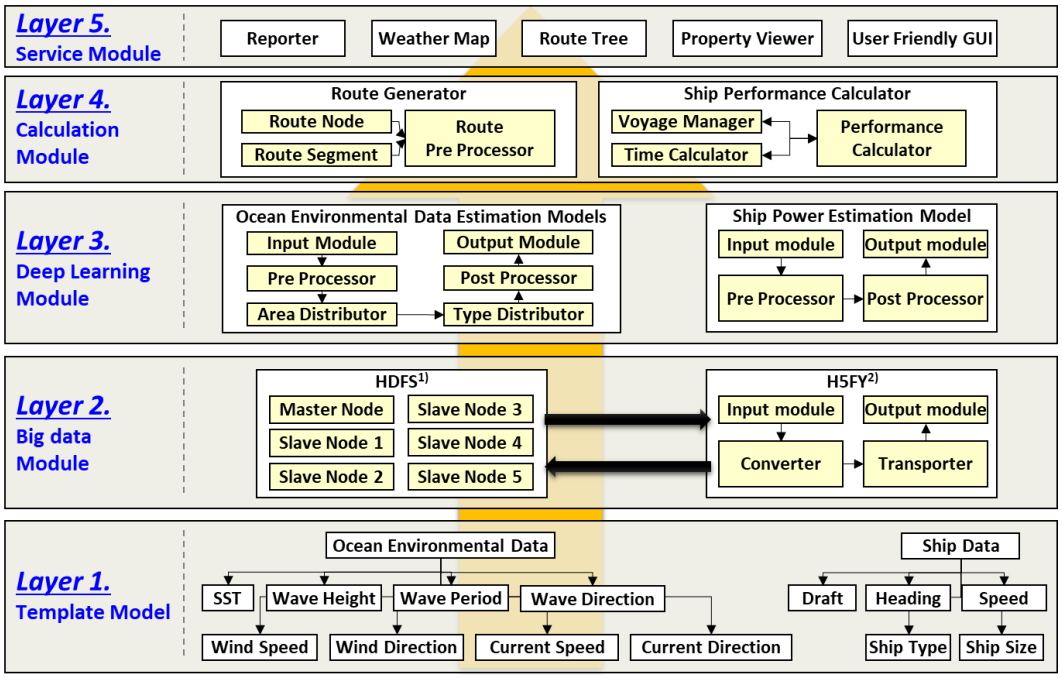

Figure 42. The internal composition of the program

The program consists of 5 logical layers. Firstly, the template model is a data structure for expressing information and routes. Also, this module process all data on the prediction of ocean environmental data and route composition. Secondly, the big data module is responsible for transmitting file input/output and request queries to and from the big data server. Thirdly, the deep learning module is in charge of data input and output required for prediction and a model for predicting ocean environmental data and ship's required power composed of python. Using the input data received from big data, it predicts the ocean environmental data and ship's required power. Fourth, the calculation module generates route information by using the ocean environmental data and ship's required power predicted by deep learning. The route information and predicted results are post-processed, and the results are sent to the GUI. Lastly, the service module visualizes the predicted

information of ocean environmental data and ship route.

5.3.3. Screen composition of the program

Figure 43 represents the screen composition of the program.

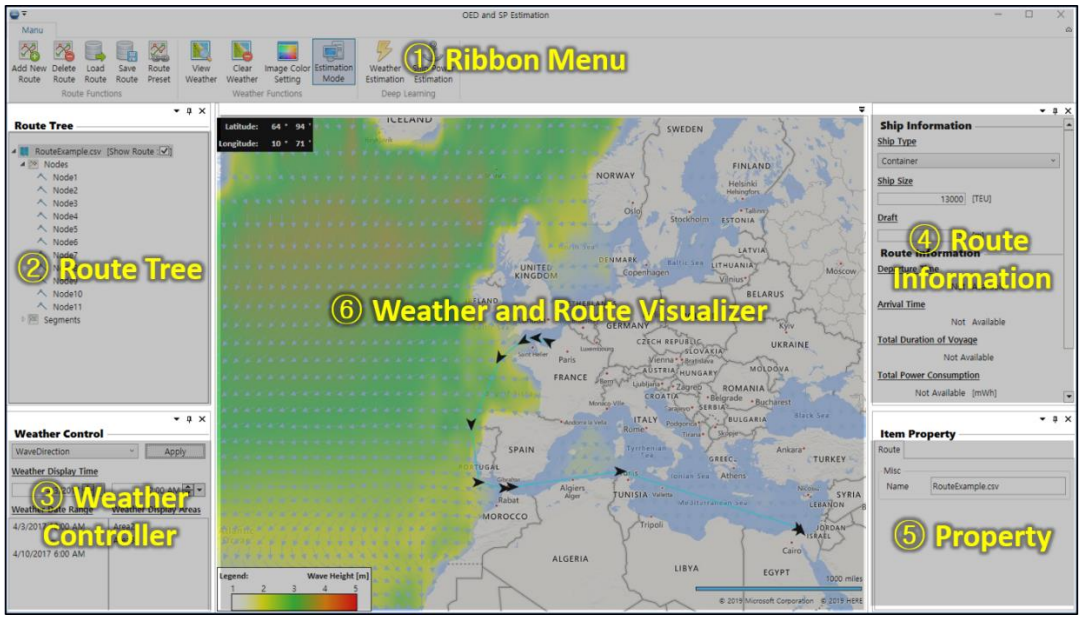

Figure 43. Screen composition of the program

The screen of the program is composed of a total of 6 compositions. The first is a collection of buttons that perform various functions required for program operation with the ribbon menu. The second is the path tree window, where you can check user-defined path information. The third is the weather control window, which displays the time range

and sea area of weather information necessary for the route, and provides a function to visualize the time and type of weather information. The fourth is the route information window, which displays information on the censer after inputting the ship's information to be used for prediction and predicting the ship's required power. Fifth, detailed information about the element (route, transit point, section) selected as a property is displayed. Lastly, the route generated by the weather and route visualizer and the desired information of ocean environmental data is expressed on the world map.

In the program, it is possible to select a ship type and ship specifications using a ribbon menu for user convenience, and select a departure date/time and execute various prediction functions. In addition, information on the selected ship's route and latitude and longitude can be grasped through the route tree window, and information of ocean environmental data, information of ship's required power, and vessel information at the selected location can be grasped through the property window. And finally, you can visually grasp information of ocean environmental data and ship's required power on the world map through the map window.

6. Conclusions and future works

In this study, a model for predicting ocean environmental data and the ship's required power was developed using deep learning. First, AutoEncoder and convolutional LSTM were used for the prediction of ocean environmental data. Using the convolutional LSTM, we were able to predict by transforming the ocean environmental data of the entire sea area into a 2D image. In addition, delayed prediction occurred when predicting ocean environmental data using LSTM and convolutional LSTM, which was solved by applying

AutoEncoder. In addition, in order to develop an optimal prediction model of ocean environmental data, the model performance was evaluated by changing the lookback range, look forward range, and channel configuration. As a result, the larger the lookback range and the smaller look forward range, the better the model performance was derived. Finally, using AutoEncoder and convolutional LSTM, a model for predicting ocean environmental data for all sea areas operated by ships was developed. Due to memory problems, the entire sea area could not be predicted at once and divided into 12 areas. For each area, a model for predicting ocean environmental data was developed. Finally, this prediction method's effectiveness was verified by comparing it with previous studies and the prediction method of ocean environmental data of the weather forecasting center.

Next, the prediction model of the ship's required power for a 13,000 TEU-class container ship using DFN was compared and analyzed. In this study, several methods were used to improve prediction accuracy. First, pre-processing of the input data was performed. Pre-processing was performed on ocean environmental data related to wind and wave, and this was compared with a prediction model that did not. Since the two results are similar, pre-processing is judged to be insignificant. Second, the structure of DFN was changed. When the structure of the DFN was changed according to the characteristics of the data (model 2), the prediction accuracy was better than that of the general DFN. Next, hyperparameters optimization was performed. Among the various elements constituting DFN, five hyperparameters that have a great influence on the prediction result were defined, and optimization was carried out. As a result, the dropout and number of hidden layers showed a significant pattern. In the case of dropout, the best prediction accuracy was obtained when no dropout was used, and in the case of the number of hidden layers, when the number of hidden layers was small. Finally, K-means clustering was performed. As a result, it was the best when the data were divided into three clusters for the ship draft, and

there was no significant progress compared to the model without K-means clustering.

In the case of ocean environmental data, the land was treated as 0 when imaged. However, since this is not a proper treatment for land, it should be treated more reasonably. In addition, the look back step is set to 12 weeks due to memory limitations, but if the computing power improves, the lookback range is increased to make a more accurate prediction. Also, in the case of the required horsepower prediction, the data of ship's required power generated based on the ISO 15016 method was used as the ground truth due to the limitation of data acquisition. If the actual data is used, a more accurate prediction will be possible. Also, in this study, the effect of K-means clustering was insignificant, but it is believed that the accuracy of prediction will improve if the criteria that affect the required horsepower are found and clustered.

Appendices

A.1 Computing power

Table 19 shows the computing power used in this study.

Table 19. Computing power used in this study

Category	Specification
CPU	Intel Xeon E5-2640 v4 (2.4Ghz) × 2EA
GPU	GeForce RTX 2080 8GB × 4EA
RAM	DDR4 32GB PC4-19200 (2400MHz) × 4EA = 128GB

A.2 Prediction result of ocean environmental data using LSTM

Figure 44 shows the prediction result of significant wave height (SWH) after one day using LSTM. In the case of SWH, it was confirmed that the predicton was made quite accurately.

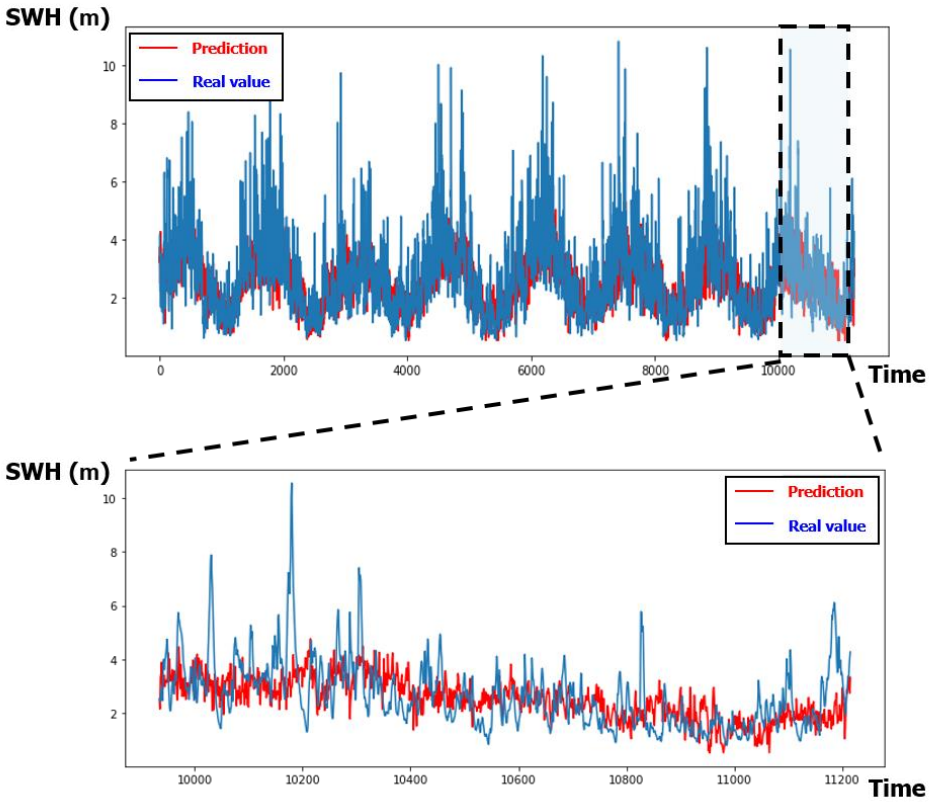

Figure 44. Prediction result of SWH using LSTM

Figure 45 shows the prediction result of the mean wave period (MWP) after one day using LSTM. In the case of MWP, it is judged that accurate predictions are not made, and only the trend is predicted.

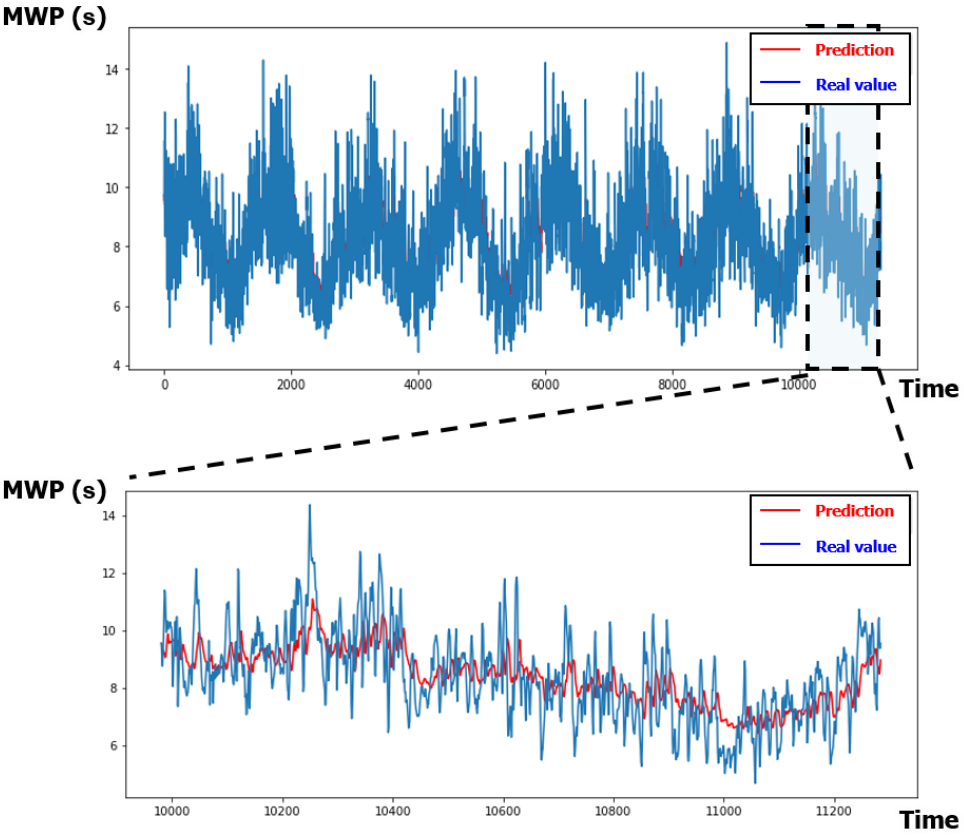

Figure 45. Prediction result of MWP using LSTM

Figure 46 shows the prediction result of mean wave direction (MWD) after one day using LSTM. In The case of MWD, the prediction was made quite accurately.

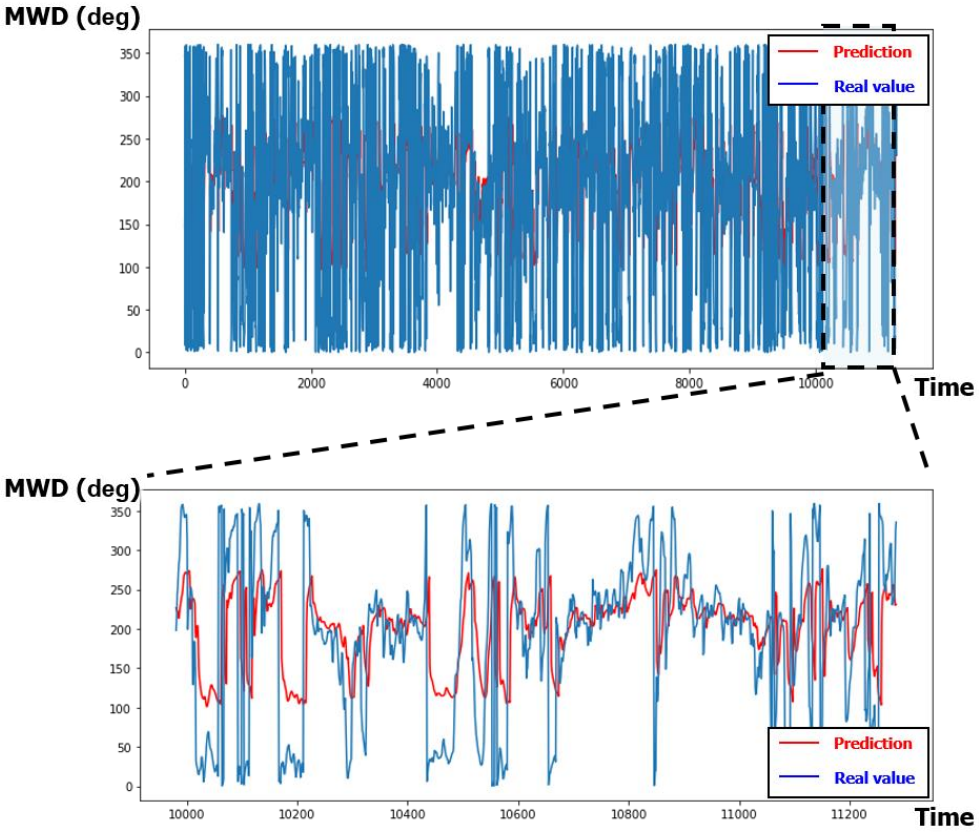

Figure 46. Prediction result of MWD using LSTM

Figure 47 shows the prediction result of current speed (CS) after one day using LSTM. In the case of CS, an accurate prediction was not made.

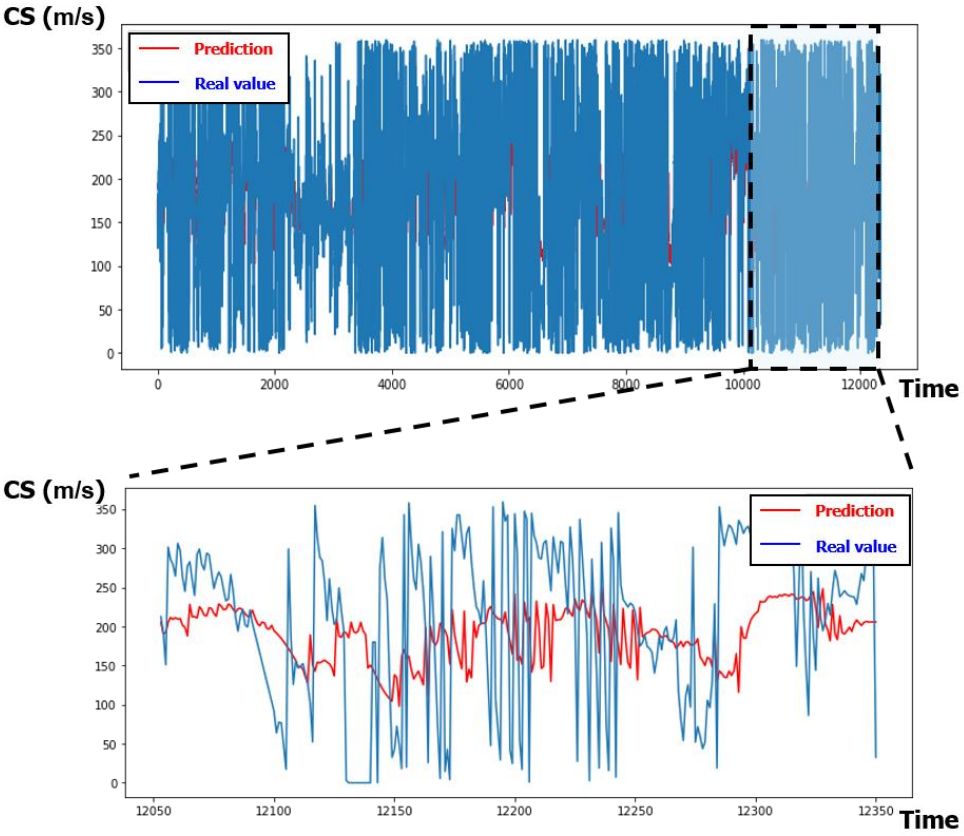

Figure 47. Prediction result of CS using LSTM

Figure 48 shows the prediction result of the current direction (CD) after one day using LSTM. In the case of CD, an accurate prediction was not made.

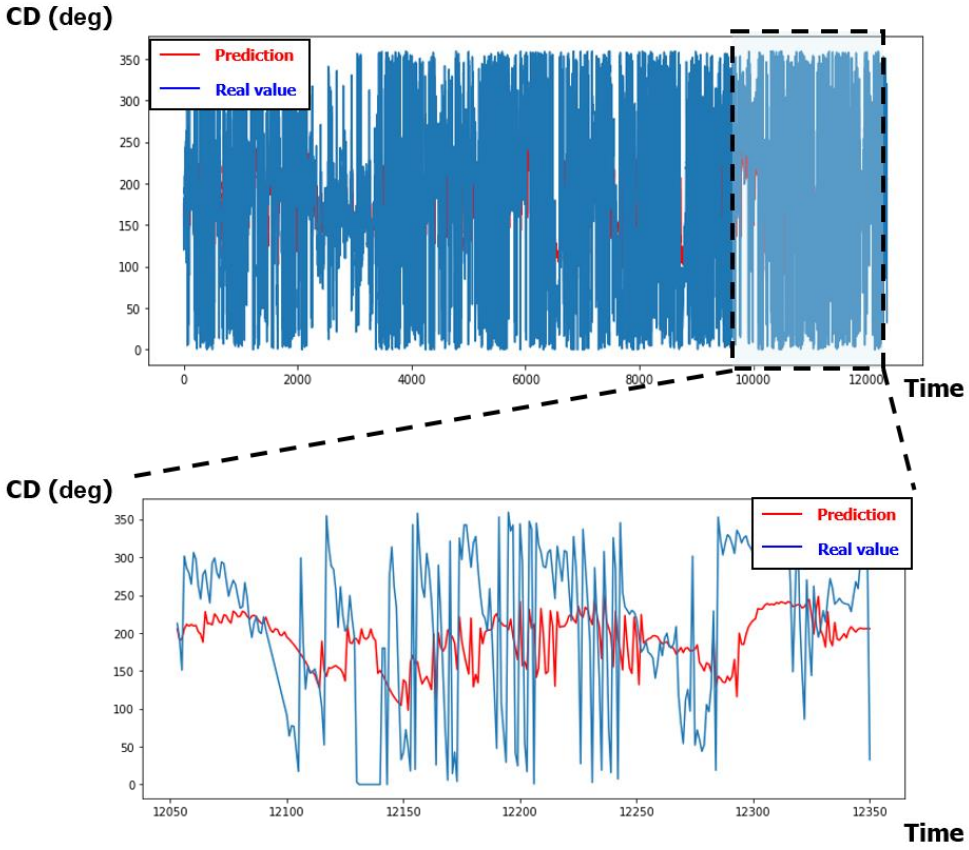

Figure 48. Prediction result of CD using LSTM

Figure 49 shows the prediction result of wind speed (WS) after one day using LSTM. In the case of WS, it was predicted accurately.

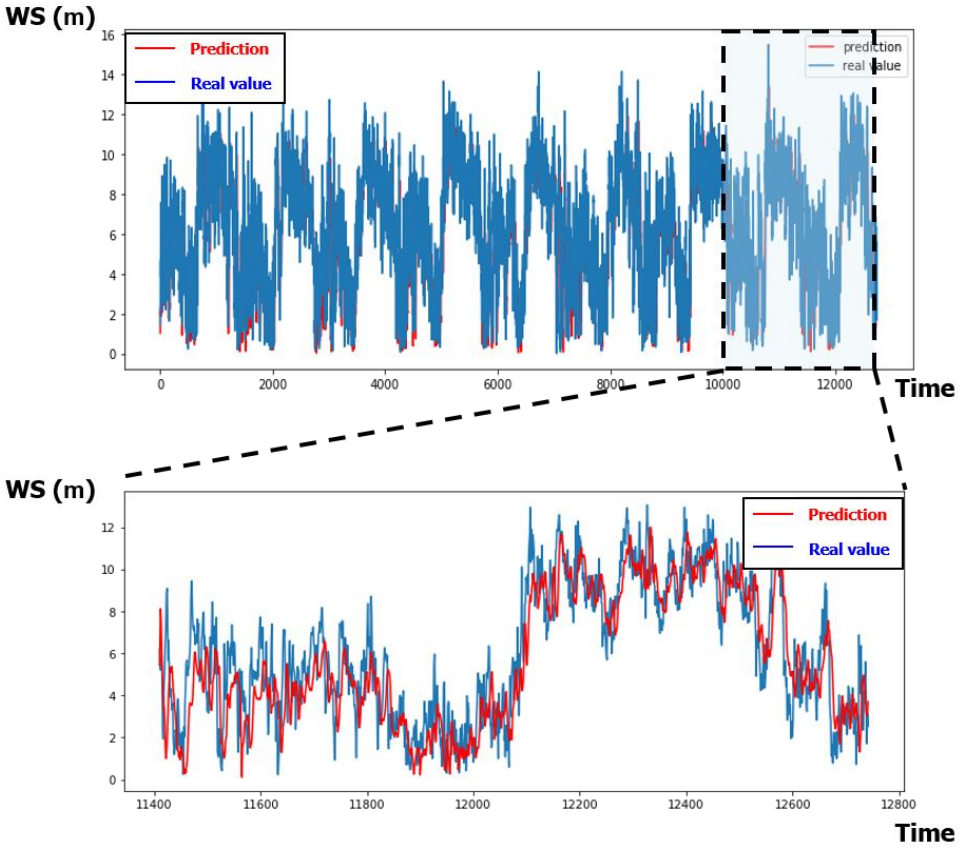

Figure 49. Prediction result of WS using LSTM

Figure 50 shows the prediction result of wind direction (WD) after one day using LSTM. In the case of WD, it was predicted accurately.

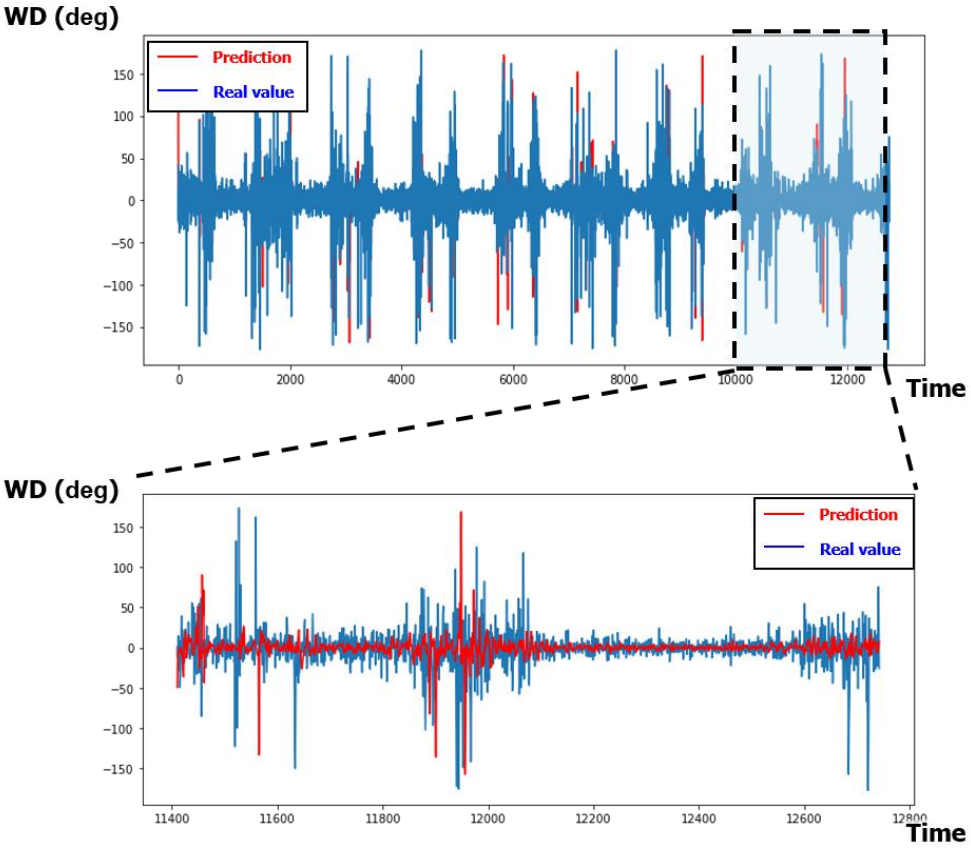

Figure 50. Prediction result of WD using LSTM

A.3 Prediction result of ship power using SVR

Figure 51 compares SVM and SVR. SVM was designed based on the concept of SVM, but there are differences due to different applications.

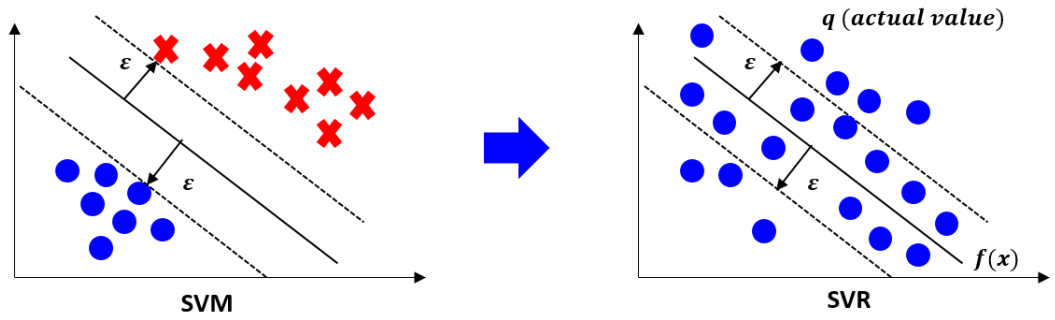

Figure 51. Comparison of SVM and SVR

SVM is to find the boundary line that best divides the data for a given ε, while SVR is to find the boundary line where as much data as possible enters ε. Therefore, SVR can be viewed as an optimization problem that minimizes the objective function of Equation (19).

$$L = \max(0, |f(x) - q| - \varepsilon) \tag{19}$$

In Equation (19), f(x) is the boundary line function, and q is the actual data. In SVR, the dimension of data is increased in order to solve the problem of finding the boundary line. In this case, the kernel function is used. There is a big difference in SVR performance depending on the kernel function. Figure 52 shows the reason for needing kernel function.

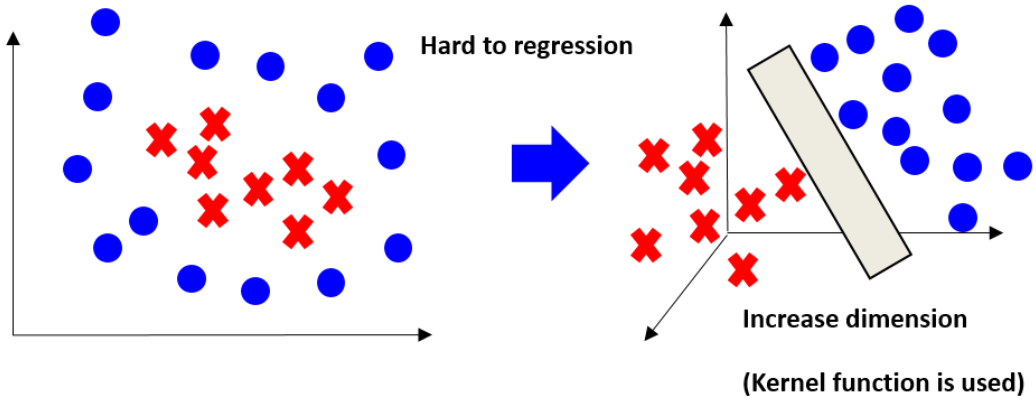

Figure 52. Reason for needing kernel function

Commonly used kernel functions include RBF (Radial Basis Function), linear, and poly functions. Figure 53 shows the prediction result of SVR (kernel function: RBF). The predicted data has a smooth distribution.

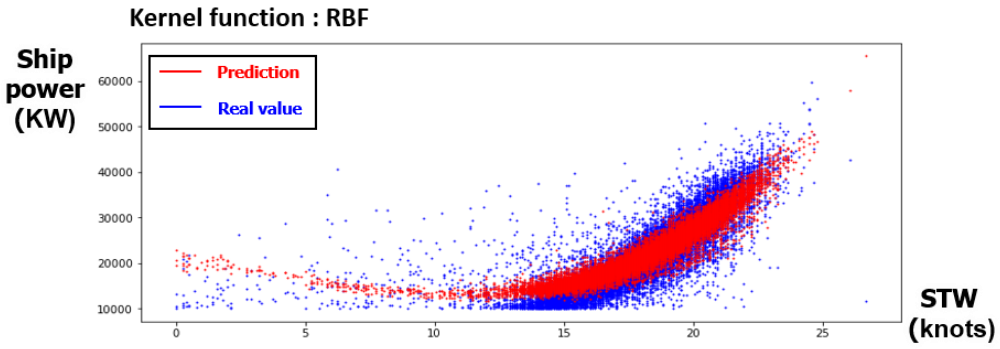

Figure 53. Prediction result of SVR (kernel function: RBF)

Figure 54 shows the prediction result of SVR (kernel function: linear). The predicted data has a linear distribution. Therefore, the prediction accuracy is low compared to other methods.

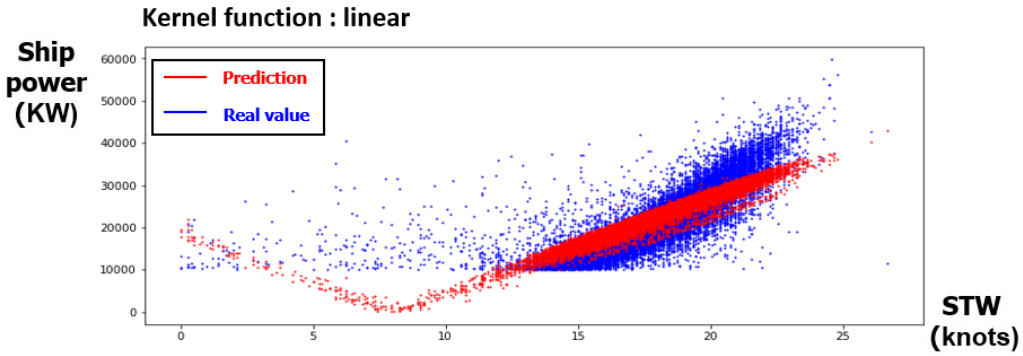

Figure 54. Prediction result of SVR (kernel function: linear)

Figure 55 shows the prediction result of SVR (kernel function: poly). The predicted data has a smooth distribution.

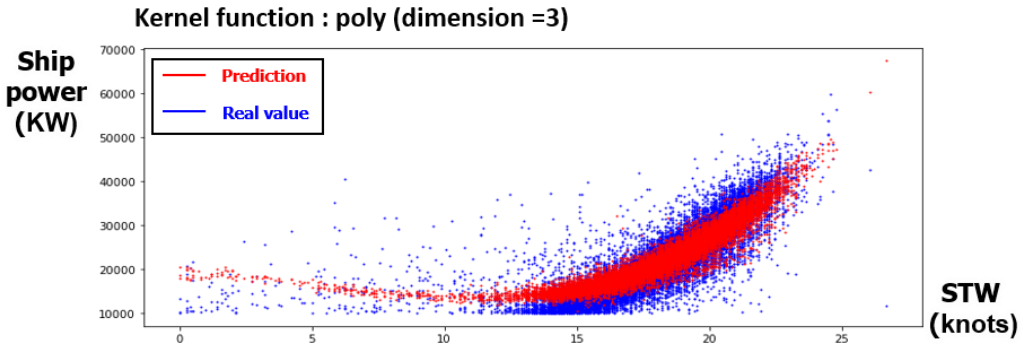

Figure 55. Prediction result of SVR (kernel function: poly)

According to the kernel function, the smoother prediction was performed when using poly and RBF functions than when using linear functions. Table 20 compares the prediction result using SVR

Table 20. Comparison of prediction result using SVR

Pre-processing	Kernel function	MAE
X	RBF	2,326 KW (4.32%)
O		2,338 KW (4.34%)
X	Linear	3,110 KW (5.78%)
O		3,118 KW (5.79%)
X	Poly	2,337 KW (4.34%)
O		2,345 KW (4.36%)

As a result, the prediction accuracy was the worst when the linear function was used as the kernel function, and the prediction accuracy was the best when the RBF was used. Therefore, in this study, RBF was used as a kernel function.

A.4 Calculation of wave spectrum

In this study, we transformed the wave spectrum for the pre-processing of the input data. When calculating the wave spectrum, the Bretschneider wave spectrum and the JONSWAP wave spectrum are mainly used [26]. The Bretschneider wave spectrum is a traditionally used method and is suitable for open sea areas. The wave spectrum equation is shown in Equation (20).

$$S_{\xi}(w) = \frac{173H_{\frac{1}{3}}^{2}}{T_1^4} w^{-5} \exp\{\frac{-692}{T_1^4} w^{-4}\} \tag{20}$$

In Equation (20), T is the mean wave period, H is the significant wave height, and w is the angular frequency. The next widely used JONSWAP wave spectrum is a method carried out on the northern coast of Sylt Island and is suitable for coastal. The wave spectrum equation was shown in Equation (21).

$$S_{\xi}(w) = \frac{320H_{\frac{1}{3}}^{2}}{T_p^4} w^{-5} \exp\{\frac{-1950}{T_p^4} w^{-4}\}\gamma^4 \tag{21}$$

In Equation (21), T is the peak wave period and γ is the peakedness factor. In this study, we use a Bretschneider wave spectrum suitable for the open sea area.

A.5 Correlation coefficient for ocean environmental data

Table 21 shows Pearson's correlation coefficient for ocean environmental data. As a result, it was confirmed that the data related to the wave (SWH, MWP) is related to the data related to the wind (WU).

Table 21. Pearson's correlation coefficient for ocean environmental data

Pearson's correlation coefficient	**SST**	**WU**	**WV**	**SWH**	**MWD**	**MWP**	**CU**	**CV**
SST	1.00	0.24	0.19	0.36	0.32	0.39	0.31	0.32
WU	-	1.00	0.03	**0.70**	0.11	0.07	0.13	0.07
WV	-	-	1.00	0.04	0.15	0.02	0.03	0.12
SWH	-	-	-	1.00	0.02	**0.68**	0.32	0.11
MWD	-	-	-	-	1.00	0.25	0.27	0.13
MWP	-	-	-	-	-	1.00	0.29	0.20
CU	-	-	-	-	-	-	1.00	0.31
CV	-	-	-	-	-	-	-	1.00

References

Bottou, L., Bousquet, O., 2009. The tradeoffs of large scale learning. Adv. Neural Inf. Process. Syst. 20 - Proc. 2007 Conf.

Draper, N.., H.Smith, 1998. Applied regression analysis 326. John Wiley Sons, New York 6221847.

Gunaydin, K., 2008. The estimation of monthly mean significant wave heights by using artificial neural network and regression methods 35, 1406–1415. https://doi.org/10.1016/j.oceaneng.2008.07.008

Harvald, S.A., 1992. Resistance and Propulsion of Ships - Harvald.

Hinton, G.E., Srivastava, N., Krizhevsky, A., Sutskever, I., Salakhutdinov, R.R., 2012. Improving neural networks by preventing co-adaptation of feature detectors 1–18.

ISO 15016, 2015. Ships and marine technology guidelines for the assessment of speed and power performance by analysis of speed trial data.

J, H., G, M., 1982. An approximate power prediction method. Int. Shipbuild. Prog. 329, 166–170.

Jain, P., Deo, M.C., 2008. Artificial Intelligence Tools to Forecast Ocean Waves in Real Time. Open Ocean Eng. J. 1, 13–20. https://doi.org/doi:10.2174/1874835X00801010013

James, S.C., Zhang, Y., Donncha, F.O., 2018. A machine learning framework to forecast wave conditions. Coast. Eng. 137, 1–10. https://doi.org/10.1016/j.coastaleng.2018.03.004

Kim, K.S., Roh, M. Il, 2020. Iso 15016:2015-based method for estimating the fuel oil consumption of a ship. J. Mar. Sci. Eng. 8, 1–18. https://doi.org/10.3390/jmse8100791

Kingma, D.P., Ba, J.L., 2015. Adam: A method for stochastic optimization. 3rd Int. Conf. Learn. Represent. ICLR 2015 - Conf. Track Proc. 1–15.

Kramer, M.A., 1991. Nonlinear principal component analysis using autoassociative neural networks. AIChE J. 37, 233–243. https://doi.org/10.1002/aic.690370209

Kristensen, H.O., Lützen, M., 2012. Prediction of resistance and propulsion power of ships. Proj. no. 2010-56, Emiss. 52.

Liang, Q., Tvete, H.A., Brinks, H.W., 2019. Prediction of vessel propulsion power using machine learning on AIS data, ship performance measurements and weather data. J. Phys. Conf. Ser. 1357. https://doi.org/10.1088/1742-6596/1357/1/012038

Lloyd, S.P., 1982. Least Squares Quantization in PCM. IEEE Trans. Inf. Theory 28, 129–137. https://doi.org/10.1109/TIT.1982.1056489

Mahjoobi, J., Kazeminezhad, M.H., 2008. Hindcasting of wave parameters using different soft computing methods 30, 28–36. https://doi.org/10.1016/j.apor.2008.03.002

Rakke, S.G., 2016. Ship emissions calculation from AIS-annotated. NTNU.

Ruder, S., 2016. An overview of gradient descent optimization algorithms 1–14.

Rumelhart, D.E., Hinton, G.E., Williams, R.J., 1986. Learning representations by back-propagating errors. Meas. J. Int. Meas. Confed. 114, 102–108. https://doi.org/10.1016/j.measurement.2017.09.025

Samsung Heavy Industries Energy efficiency management system, 2016.

Shi, X., Chen, Z., Wang, H., Yeung, D.Y., Wong, W.K., Woo, W.C., 2015. Convolutional LSTM network: A machine learning approach for precipitation nowcasting. Adv. Neural Inf. Process. Syst. 2015–Janua, 802–810.

Uyanik, T., Arslanoglu, Y., Kalenderli, O., 2019. Ship Fuel Consumption Prediction with Machine Learning. 4th Int. Mediterr. Sci. Eng. Congr. 1–7.

Vapnik, V.N., 2000. The Nature of Statistical Learning Theory, The Nature of Statistical Learning Theory. https://doi.org/10.1007/978-1-4757-3264-1

Werbos, P., 1974. Beyond Regression : New Tools for Prediction and Analysis in the Behavioral.

Yoo, B., Kim, J., 2017. Powering performance analysis of full-scale ships under environmental disturbances. IFAC-PapersOnLine 50, 2323–2328. https://doi.org/10.1016/j.ifacol.2017.08.474

Zhang, Q., Wang, H., Dong, J., Zhong, G., 2017. Prediction of Sea Surface Temperature Using Long Short-Term Memory 14, 1745–1749.

국문 초록

딥 러닝을 이용한 해기상 및 소요 마력 예측 모델 개발

선박의 소요 마력을 최소로 하는 경제 항로를 결정하기 위해서는 해기상의 예측과 그에 따른 소요 마력 예측이 필요하다. 해기상 예측 데이터를 제공하는 European Centre for Medium-Range Weather Forecast (ECMWF), Hybrid Coordinate Ocean Model (HYCOM)과 같은 기상 정보 업체는 일반적으로 6 주 정도의 단기 예측을 진행한다. 따라서 장기 예측이 필요할 때는 해기상 정보를 자체적으로 예측해야 한다. 소요 마력 예측의 경우에 전통적으로 모형 실험 결과를 활용한 numerical method 가 많이 활용되고 있다. 그러나 이러한 방법은 모형 실험의 불확실성 때문에 실선의 소요 마력을 정확하게 예측하기 어렵다. 이러한 문제를 해결하기 위해 실선 테스트를 진행해야 하지만, 이는 많은 비용과 시간이 소모된다. 따라서 본 연구에서는 딥 러닝을 활용하여 해기상 및 소요 마력을 예측하였다.

해기상 예측과 관련하여 많은 연구들이 딥 러닝을 활용하였다. 그러나 대부분은 파고, 파 주기, 파향 등 제한적인 해기상 데이터에 대한 예측을 진행하였다. 또한 전 해역이 아닌 특정 해역에 대해 예측을 진행한다는 한계점이 있었다. 따라서 본 연구에서는 전 해역에 대한 해기상 예측을 위해 전 해역의 해기상을 이미지화 하였다. 추가로, 이러한 시계열 이미지 데이터를 학습하는데 적합한 convolutional LSTM 을 활용하였다. 또한 시계열 데이터 예측 문제에서 주로 발생하는 delayed prediction 을 해결하기 위하여 AutoEncoder 를 활용하였다. 또한 최적의 모델을 찾기 위해 Input data 의 크기 (look back range), output data 의 예측 시점 (look forward range) 등을 변경하여 모델의 성능을 평가하였다. 최종적으로 이러한 모델을 바탕으로 전 해역을 12 개의 area 로 구분하여 해기상 예측을 진행하였다.

소요 마력 예측과 관련하여 많은 연구들이 regression analysis 를 활용하였다. 그러나 regression analysis 는 해상 및 선박 운항 상태에 영향을 받는 소요 마력 예측 문제와 같은 복잡한 문제의 경우 예측 정확도에 한계를 보였다. 따라서 본 연구에서는 수치 예측에 적합한 딥 러닝 모델인 DFN 을 활용하였다. 또한 예측 정확도를 높이기 위해 다양한 방법을 활용하였다. 첫번째로, 해기상 데이터에서 wind 와 wave 관련 데이터의 경우 선박에 대한

상대 수치로 pre-processing 을 수행하여 그 효과를 확인하였다. 두번째로, DFN 의 입력 데이터의 특성에 맞게 DFN 의 모델 구조를 변경하여 그 효과를 확인하였다. 세번째로, DFN 학습 모델을 위한 number of hidden layers, number of hidden nodes, learning rate, dropout, gradient optimizer 의 5 가지 hyperparameters 의 조합에 따른 예측 정확도를 분석하였다. 네번째로, 해상 및 운항 상태에 따른 독자적인 선박의 소요 마력 예측 모델을 개발하기 위해 K-means clustering 을 진행하였다. 이와 같이 다양한 소요 마력 학습 모델의 성능 및 그 이유를 비교 분석하였다.

Keywords: Ocean environmental data, ship’s required power, DFN (Deep Feedforward Neural network), Convolutional LSTM (Long Short-Term Memory), AutoEncoder

Student number: 2018-24953